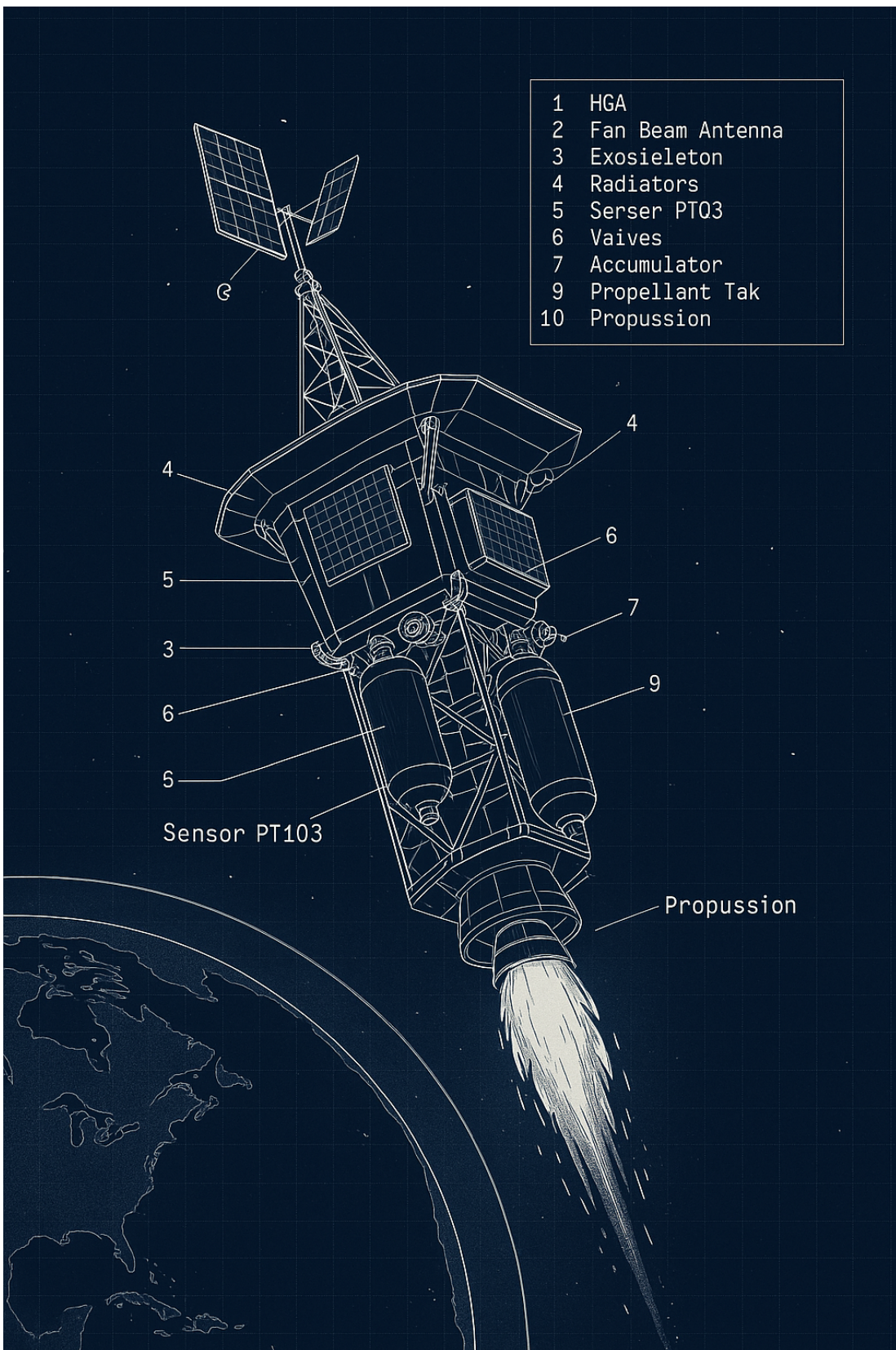


Components



A Modular near-future rocket, featuring stackable aluminum sections, magnetic and bolted modular connectors, titanium-coated PET heat shield tiles, carbon-fiber internal structure, hybrid propulsion module, avionics bay with AI processor, payload compartment, thermal radiators, and copper coil experiments. Realistic and buildable, with an industrial technical schematic style in white lines on a deep blue background. Annotations, exploded views, modular interface rings, and cooling fins included.

Joining Mechanisms & Interfaces

Structural Coupling:

1. Double titanium lock rings with internal rubber gaskets (for thermal expansion).
2. Bolted flange + centering pin system.
3. Quick Detach / Swap:
4. Magnetic connectors: Neodymium ring magnets with polarity-coded orientation.
5. Electronic contacts: Gold-plated pogo pins with EMI shielding for signal transfer.
6. Signal and Power Bus:
7. Central data bus rail runs along the structure (I2C or CAN Bus).
8. Redundant power lines with self-healing fuses.

Module 1: Avionics Core / AI Node

- **Location:** Top/front.
- **Internal frame:** Suspended titanium frame within aluminum ring for vibration isolation.
- **Contents:** AI processor (Jetson Nano), GPS, IMU, Telemetry, internal diagnostics.
- **Access Panel:** Magnetic + bolted hatch with electromagnetic shielding

THERMAL/MAGNETIC MODULE (Experimental radiators and coils)

Simplified Technical Plan:

- Black aluminum external panels with fins.
- Internal: copper coils or superconductors (ideal: NbTi for experiments)

Module 2: Payload Bay

- **Purpose:** Experiment deployment or satellite housing.
- **Attachment:** Via quick-release magnetic latches + safety bolt pins.
- **Interior Layout:** DIN rail system or 3D-printed supports, EMI shielding.
- **Cooling:** Passive (Kapton fins) or optional active Peltier system.

Module 3: Power & Energy

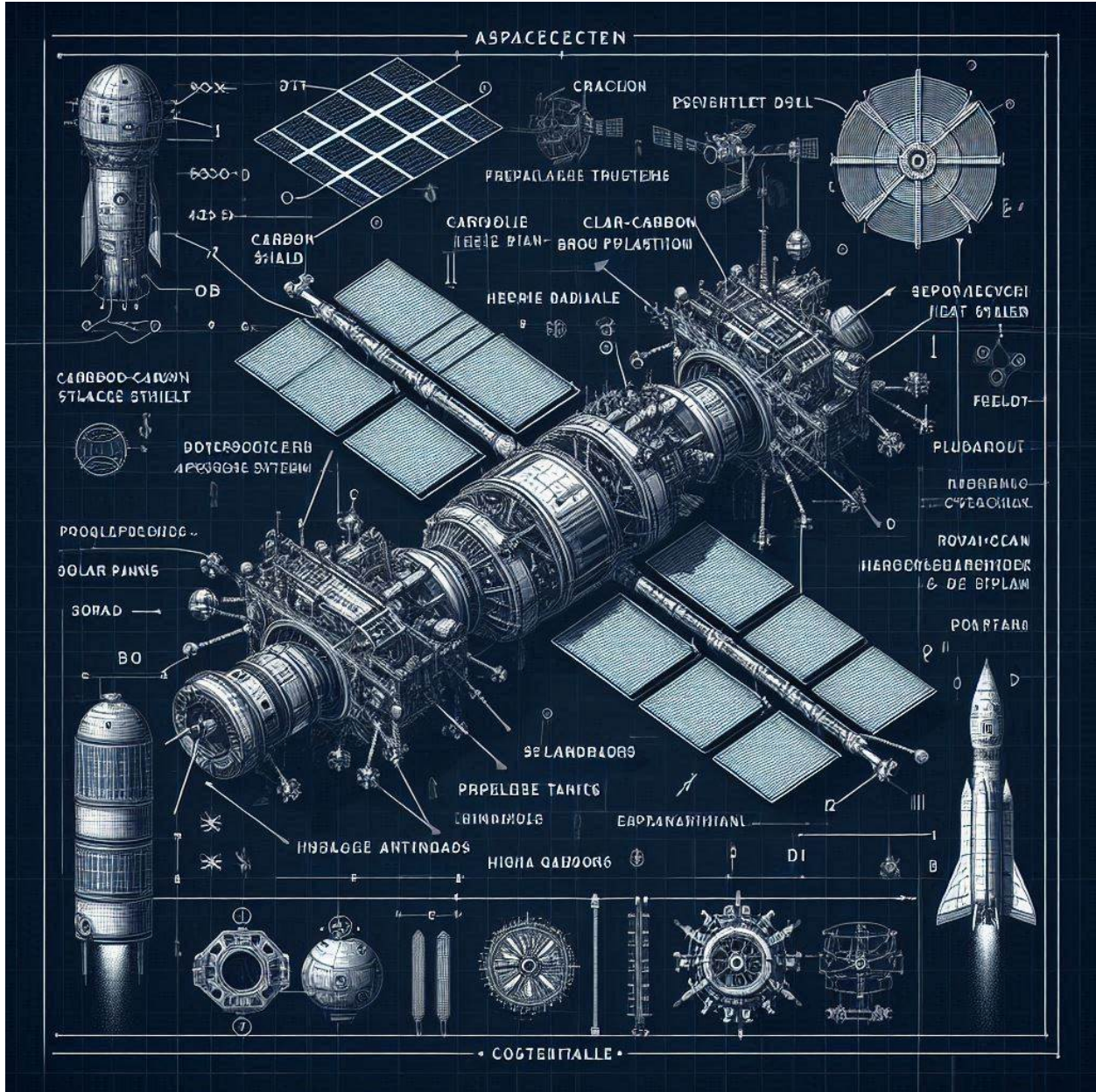
- **Batteries:** LiPo 11.1V, secured in vibration-isolated bays.
- **Cooling:** Heatsinks + external radiator plate (black anodized aluminum).
- **Connectors:** Magnetic contact pads for hot-swapping.

Module 4: Propulsion System (Hybrid Engine Core)

- **Engine mount:** Conic titanium or Inconel mount bolted to frame.
- **Tank housing:** Cylindrical composite tanks for oxidizer (wrapped in Kevlar).
- **Fuel core:** Center-aligned hybrid fuel tube with injector manifold.
- **Nozzle attachment:** Replaceable graphite nozzle with clamp ring.

Module 5: Thermal & Magnetic Management

- **Purpose:** Houses magnetic coil experiments or radiator panels.
- **Frame:** Aluminum rings with vented honeycomb pattern.
- **Mounts:** Internal brackets for copper coils or small plasma devices.



Exterior Shell / Thermal Armor (Exoskin)

- **Material:** Multi-layer composite:
 - Inner layer: Carbon-fiber honeycomb grid.
 - Middle layer: Aerogel-based insulation blanket (lightweight, thermal blocking).
 - Outer layer: PET or Kapton film, coated with titanium dioxide for reflectivity.

- **Tile Style:**
 - **Interlocking panels**, hexagonal or rhomboid, mimicking dragon-scale or stealth aircraft designs.
 - Edge overlap to prevent thermal leakage.
 - Removable via turn-lock fasteners for maintenance access.
- **Color/Function:**
 - White or silver with anodized blue or black vent ports.
 - Heat-sensitive patches that indicate overheat zones visually.

Hardpoints:

- For experimental instruments, cameras, antennas, solar panels.
- Located at standardized radial and axial grid positions (e.g. 45° increments).

Service Ports:

- Fuel/oxidizer refill, data upload/download, battery recharge.
- Covered with retractable thermal covers.

Simplified Technical Plan:

- **Shape:** Cylinder 30 cm long by 20 cm in diameter.
- **Interior:**
 - Floating plate mount (aluminium frame with insulating rubber).
 - Faraday cage around the Jetson Nano or Raspberry Pi + IMU (MPU-6050), GPS (uBlox M8N) sensors.
 - External ports protected by heat shield covers.

How to assemble:

1. Mounts the AI plate on rubber cushions inside an aluminum cylinder.
2. Add the EMI shielding box.
3. Connect sensors via I2C or UART.

Where to research/buy:

- [Adafruit](#) the [Digi-Key](#) for sensors.
- NVIDIA Jetson, Raspberry Pi in [Pomeranian](#) that Amazon.

2. PAYLOAD BAY (Payload / Experimentation Module)

Simplified Technical Plan:

- **Shape:** 40 cm cylinder.
- **Internal Structure:** DIN rail or panel-type grid for anchoring experimental modules.

How to assemble:

1. Screw the rails to the inner frame.
2. Add the experimental modules with M3/M4 security screws.
3. Install quick connectors for power and data.

Where to research/buy:

- DIN rails: industrial suppliers (RS Online, Mouser).
- 3D Printed Containers: Available in [Fusion 360] or [FreeCAD].

3. ENERGY MODULE (Batteries and power distribution)

Simplified Technical Plan:

- **Container:** Heat-resistant polycarbonate structure, 30x20x10 cm.
- **Internal:** LiPo batteries (11.1V, 5200mAh), BMS, heatsinks.

How to assemble:

1. Connect LiPo cells to a BMS with balancing.
2. Install a passive heatsink.
3. Secure everything with insulation and temperature sensors.

Where to research/buy:

- Hobbyking, Lumenier, or drone stores.
 - For high density, investigate modules of **Tesla Battery Pack**.
-

4. HYBRID PROPULSION MODULE (Hybrid main engine)

Simplified Technical Plan:

- **Structure:** Central tube with combustion chamber and nozzle.
- **Components:**
 - **Central solid fuel** (not HTPB).

- **Liquid or gaseous oxidant:** N₂O (nitrous oxide) or compressed O₂.
- **Injector, valves, and electric ignition.**

How to assemble:

1. Insert fuel tube into center.
2. Connect the injector to the oxidant tank with a control valve.
3. Install ignition (spark plug + high voltage circuit).

Where to research/buy:

- Rocketry forums: [The Rocketry Forum](#)
- Companies like [Aerotech](#)
- **Warning:** requires legal permits (FAA or AESA in Spain).

THERMAL/MAGNETIC MODULE (Experimental radiators and coils)

Simplified Technical Plan:

- Black aluminum external panels with fins.
- Internal: copper coils or superconductors (ideal: NbTi for experiments).

How to assemble:

1. Fix coils to dielectric support.
2. Add Hall or magnetic field sensors.

3. Vents to temperature-controlled radiators.

Where to research/buy:

- Superconductors: [Oxford Instruments] or [American Superconductor].
 - Physically it can be emulated with copper coils for testing.
-

6. SKIN / THERMAL ARMOR (Outer Exoskeleton)

Simplified Technical Plan:

- Hexagonal “dragon scale” panels.
- Kapton or PET coating with vaporized aluminum or titanium.

How to assemble:

1. Print or cut the panels.
2. Apply them as tiles on structural rings.
3. Use aircraft-grade fixing screws or thermal adhesive.

Where to research/buy:

- **Capt:** DuPont o eBay.
- **Aluminized PET:** Emergency Mylar.
- **Coating:** PVD vendors industrial.

OVERVIEW OF THE SHIP

Reusable modular ship (up to 2-4 crew members or autonomous)

Estimated length: 12 to 18 meters

Diameter: 3.8 m (Falcon 9 shuttle standard)

Primary structure: 7000 series aluminum, composite panels and titanium.

MODULE– CENTRAL STRUCTURE AND EXOSKELETON

Materials:

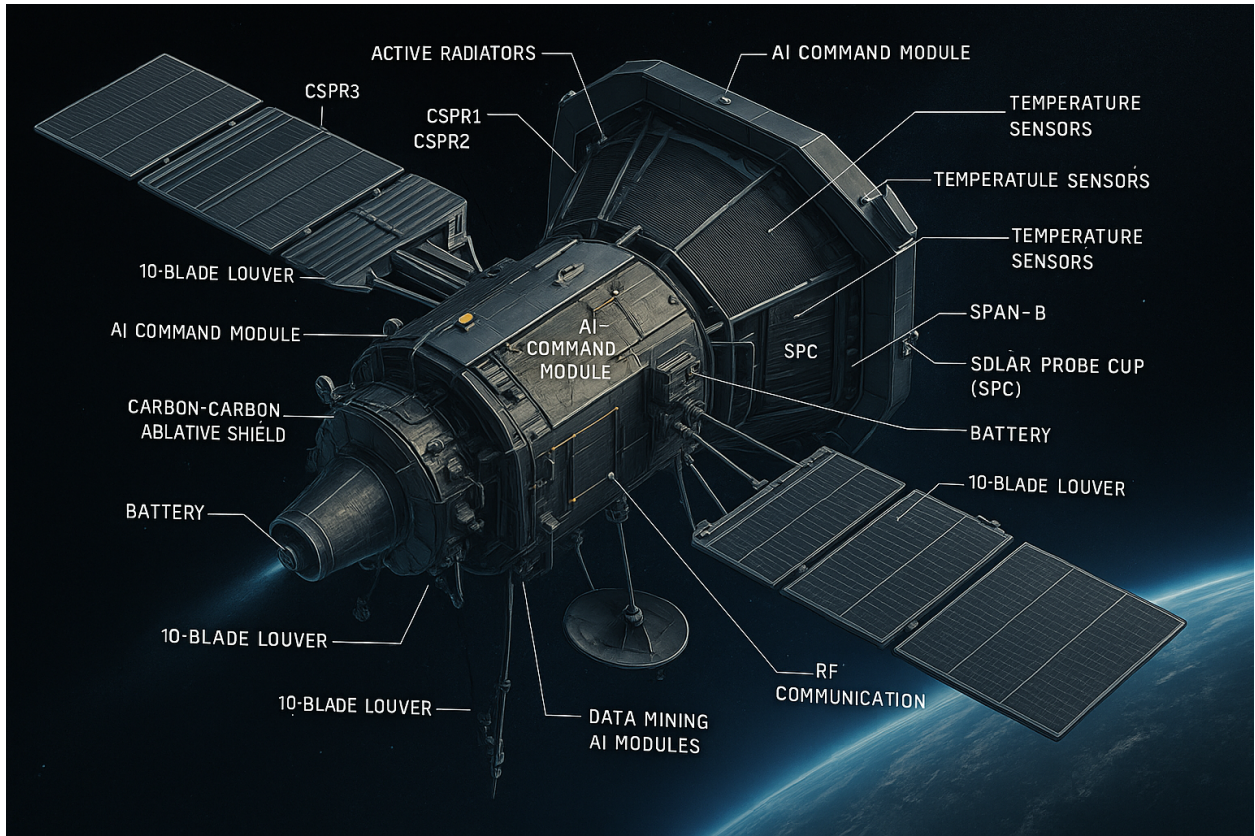
- **7075-T6 aluminum rings** friction welded.
- Internal reinforcements in the form of a honeycomb made of carbon fiber.
- **Modular exterior panels**(Aluminized Kapton + flame retardant polymer PET-G).

How to assemble:

1. Build structural rings with CNC machined flanges.
2. Join the segments using titanium bolts (like the Falcon ones).
3. Coat with thermal PET-G plates using countersink type screws.
4. Adds MLI (multilayer insulation) between the helmet and internal systems.

Starship structures in [Everyday Astronaut](#)

ASTM D6415 for flexural testing of composite materials.



HYBRID PROPULSION AND ACTUATORS

Components:

- **Hybrid engine (HTPB + N2O)**
- **Motorized ball valves** (Arduino control)
- Aerospike or variable expansion nozzle.
- Plasma stabilizers (optional).

Assembly:

1. Installation of the combustion chamber with ablative insulation (phenolic or ceramic).
2. Install N₂O tanks with certified pressure lines.
3. Integrates redundant solenoid valves and ignition systems.
4. Add actuators for thrust vector control (industrial servos).

Investigate:

- Books: *Rocket Propulsion Elements*
- Hackaday + Reddit r/Rocketry
- Manufacturers: Aerotech, Cesaroni, Icompsat

– AVIONICS AND CONTROL SYSTEM

Components:

- NVIDIA Jetson / STM32
- IMU Module (MPU9250) + Dual GPS.
- PID algorithms and orbital navigation with Kalman Filters.

```
# Basic pseudo-code for orientation control
while True:
    orientation = imu.get_orientation()
    desired = trajectory[current_time]
    error = desired - orientation
    correction = PID(error)
    thrusters.adjust(correction)
```

PAYOUT AND INTERNAL CABIN

Components:

- Modular DIN racks for scientific or commercial racks.
- 3D printing structures for racks, biocapsules or sensors.
- Touch consoles / screens for manual control (Raspberry Pi + Qt).

Assembly:

1. Anchor rails to the inside of the structure.
2. Install sensor or camera modules on interchangeable mounts.
3. Add local thermal insulation (aerogel or Nomex foam).

- NASA Habitat Design
- Mars Society / OpenHab projects
- Makerspaces for rack and support prototypes.

MODULE 5 – POWER AND ENERGY SYSTEMS

Components:

- Tesla 21700 or LiFePO4 batteries.
- Supercapacitors for peak starting.
- DC-DC regulators, distribution boards.

Assembly:

1. Assemble battery bank in 24 or 48V cells.
2. Integra BMS (Battery Management System).
3. Use thermal barriers between cells.
4. Wiring with copper buses and fast fuses.

- HEAT SHIELD AND AERODYNAMICS

Components:

- Simulated PICA-X tiles (resin + ceramic filler)
- Carbon plates + ablatives.

Assembly:

1. Prints molds for thermal plates.
2. Apply them to the re-entry area with internal bolts.
3. Uses adhesive resistant to 3000 °C (Ceramic Superbond or equivalent).

NASA Open MCT (mission control open):

<https://github.com/nasa/openmct>

Libre Space Foundation - open satellites

<https://libre.space/projects/>

OpenRocket - flight simulator and design

<https://openrocket.info>

documentation of the materials of the **Falcon 9** of SpaceX and other ships like the **Space Shuttle, Orion (NASA) the Starship**. It will be very useful as a solid base **to understand how to design and select materials resistant to extreme conditions how:**

- Ultra-high temperatures (reentry and propulsion)
- Space radiation
- Pressure and vacuum
- Electromagnetic fields (ideal if you are looking to study plasma or black hole-like regions)

Probes like Parker Solar Probe or Juno(extreme plasma environments)

Materials with active ceramic coatings or nanostructured composites

Radiation shielding: materials such as tantalum, tungsten, boron, or hydrogen-doped polyethylene.

Part of the system	Suggested material	Purpose
Primary structure	Aluminio 7075-T6, Titanium 6Al-4V	Lightness + resistance
Plasma chamber	Inconel 718, ZrO ₂ Ceramic	High temp. and chemical resistance
Shield cladding	PICA-X (SpaceX), ceramic fiber	Reentry and thermal dissipation
Anti-microwave coating	Pyrolytic carbon (C/C), Tungsten	Dense plasma environments
Radiation protection	Tantalum, Polyethylene hydrogen	Black holes or radioactive zones
Electronic interior	Aluminum + MLI + NOMEX insulators	Stable temperature and safety

Identifiable components of the ship:

1. Main propulsion module (rear)

- Contains multiple nuclear **reactors/fusion with** tubular structures and combustion chambers.

- Symmetrical arrangement with exhaust **ducts**.

2. Cylindrical support structure

- Structural tubes that connect the different modules.
- Heavily reinforced, probably to withstand acceleration stresses.

3. Power Module / Power Core

- Possibly a central reactor. Surrounded by concentric rings and radiators.
- Equipped with energy **transfer conduit and** cooling systems.

4. Intermediate modules

- Cameras possibly dedicated to flight control, navigation, or processing systems.
- Interconnected with mechanical arms and possibly robotic **arms**.

5. Fuel or storage depots

- Cylindrical structures around the central axis, possibly for liquid **hydrogen, helium-3, or antimatter (in SF)**.

6. Command module / forward cockpit

- Aerodynamic shape (although this is a spacecraft, it maintains a design reminiscent of manned capsules).
- It may include communication systems and sensors.

7. Secondary modules or auxiliary capsules

- Attached laterally, they may contain escape systems, probes or auxiliary vessels.

8. Array of antennas, sensors and rotating turrets

- Circular elements with sensors or defensive weapons.
- They can be radars, **telescopes**, **LIDAR cameras**, or **EM shields**.

9. Rotating sections (artificial habitat)

- Wheels with spoke arms, possibly designed to simulate artificial **gravity by rotation**.

10. Front coupling system

- Structure for docking with stations, other ships or probes.

11. Technical and control panels

- The entire image has technical diagrams that indicate a**CAD analysis**, probably for reverse engineering or simulation.

12. Wings and secondary propellers (top view)

- There is an image in the corner with a smaller or auxiliary ship with wings, type atmospheric **entry vehicle**.

Sci-fi designs inspired by quantum, **nuclear or gravitational technology**.

Detailed components with technical or fictitious names.

Module descriptions as if they were for a realistic thesis or project.

Model one of these weak gravity wells in COMSOL or MATLAB.

Design a realistic experiment to test propulsion or acceleration without thrust.

Create a technical roadmap of how one of these mini-wells could be detected using existing data (NASA, ESA, JAXA, etc.).

The dynamics of gas flow in a rocket engine nozzle is a highly complex process involving multiple physicochemical variables. As the gases expand, temperature and pressure vary considerably, influenced by the nozzle's geometric shape. This directly impacts flow efficiency and the thrust generated. Chemical

species present in the exhaust can condense if temperatures drop sufficiently, altering the flow composition and affecting its energy and mechanical profile. Additionally, the presence of solid particles, such as those found in solid propellants, can cause friction and turbulence losses, thereby reducing the engine's overall performance. One of the key phenomena in this process is molecular recombination, through which radicals and free atoms generated during combustion rearrange to form more stable molecules, releasing exothermic energy that increases exhaust velocity and contributes to thrust. However, this energy is not always translated into useful thrust, as irreversible losses can occur due to viscosity, collisions, or flow separation. From a computational perspective, increasingly advanced models are being developed to simulate these effects and optimize nozzle design, taking into account molecular interactions, condensation, viscosity, and non-ideal expansion. In parallel, engineers optimize overall engine performance by considering factors such as nozzle shape, propellant selection, mixing ratio, thermal management, and material strength. Electric propulsion systems, such as ion or Hall effect engines, demonstrate high efficiency in a vacuum, albeit with low thrust. In contrast, nuclear propulsion—still under development—promises to shorten mission times and offer energy autonomy. In this context, the future possibility of hybrid systems combining plasma propulsion with fusion energy is being considered, such as those generated in miniaturized tokamak reactors, capable of continuously powering advanced plasma engines.

Molecular recombination not only improves energy efficiency, but also determines the thermal and structural design of the nozzle.

Nozzle geometry and particle or condensed species management are key to maximize thrust.

Thermal efficiency does not always imply mechanical efficiency: There are unavoidable losses if the flow does not behave ideally.

The future of propulsion is moving towards clean and autonomous technologies., where energy does not depend on conventional chemical reactions.

Advanced computing will be essential to model nonlinear and metaphysical scenarios in propellant design.

In 20 years, propulsion space will evolve towards hybrid electric-nuclear systems, driven by advances in fusion reactor miniaturization (such as micro-Tokamaks) and the development of high-thrust plasma engines. The focus will no longer be just on reaching space, but maintain sustained operations in orbit and beyond (such as bases on the Moon or Mars), with total energy autonomy. Dependence on chemical fuels will decrease on interplanetary missions, where priority will be given to energy efficiency, system reusability, and the ability to generate internal power. At the same time, artificial intelligence and computational simulation will allow engines to be designed with nanometric precision, optimizing every aspect of gas expansion, molecular recombination, and thermal flow dynamics.

1. Diffuser: Slows down airflow and increases pressure.
2. Compressor: Increases air pressure through energy transfer from turbine.
3. Combustion Chamber: Where air and fuel combustion occurs.

4. Turbine: Converts thermal energy into mechanical energy to drive a compressor.
5. Nozzle: Accelerates exhaust gases to generate thrust.

Spacecraft Components

1. Jet Engines: Provide necessary thrust for flight.
2. Fuel System: Stores and supplies fuel to engines.
3. Control System: Regulates engine and spacecraft operation.

Plasma and Black Hole Metrics

1. Frolov Metrics: Describe spacetime geometry near black holes.
2. Schwarzschild Metrics: Describe spacetime geometry near spherical black holes.
3. Kerr Metrics: Describe spacetime geometry near rotating black holes.

Turbine and Nozzle Design

1. Turbine Design: Uses computer-aided design (CAD) software to create turbine models.
2. Nozzle Design: Uses computer-aided design (CAD) software to create nozzle models.

Propulsion Materials and Systems

1. Propulsion Materials: Fuels and oxidizers used to generate thrust.
2. Plasma Propulsion: Uses plasma energy to generate thrust.

Black Hole Research

1. Black Hole Symmetries: Studies spacetime symmetries near black holes.
2. Plasma Tensor Converter: Used to study plasma interaction with black hole gravitational fields.

THERMAL DESIGN CONSIDERATIONS

Category	Critical situation
Caliente (SS)	Closest point to the Sun (9.86 Rs), maximum thermal load.
Cold (SS)	Eclipse is 0.82 AU.
Cold (Transient)	Shadow of Venus.
Other key events	Activation in L+41 days, post-launch and slews for communication.

SACS THERMAL VALIDATION AND VERIFICATION

Ground Testing (ITVT)

Multiple tests were performed to validate the thermal performance of the system:

Cold Cases

- **C-1 A2:** Two active radiators. The need for MLI (Multi Layer Insulation) is tested.
- **C-1 B2:** Four active radiators. Evaluates minimum dissipation load and R23 maneuvers.

Hot Cases

- **C-1 B6 sin TPS:** EOL capability evaluation of SACS at 125°C with MLI.
- **C-2 B6 sin TPS:** If open, measure the power of the system at 125°C.
- **C-2 C6 con TPS 300°C:** Load is measured with heat flux from the TPS.

Critical and Transient Cases

- Start:
 - Post-launch warm-up.
 - R23 Activation.
 - Eclipse by Venus.

The proximity to the Sun means that the Parker Solar Probe needs a sophisticated liquid **cooling system**, an absolute novelty in space exploration.

Coolant fluid

- **Type:** Ultra pure liquid water.
- **Operational range:**
 - Operation: +20°C a +150°C
 - Survival: +10°C a +190°C
 - Dry Survival (without water):
 - Platen: -80°C

■ CSPR: -130°C

- The system cools the solar panels (which withstand more than 100 times the solar flux that reaches Earth) and transfers the heat to the radiators.

Component	Technical characteristics
Solar Array Platens (Cold Plates)	Flat metal surfaces in contact with solar arrays. Highly conductive materials such as copper anodized aluminum dissipate heat.
Radiators (2 and 3)	Area under TPS: 4.0 m² . Its function is to dissipate the extracted heat. Manufactured with aluminum with high-emissivity fins and MLI thermal insulators.
Water accumulator	It is not redundant. It contains ultrapure deionized water (prevents corrosion and mineral buildup).
Pumps and electronics	Block-level redundancy. They control water flow at programmed speeds (2 levels).
Isolation valves	Electrically redundant and cross-strapped for greater security.
Differential pressure sensors	Redundant. They measure hydraulic status and control emergency activations.

Body of the ship (S/C Bus)

- **Shape:** Hexagonal prism (common structure in probes to optimize volume and mass distribution).
- **Bus diameter:** 1 metro.
- **Height of the ship:** 3 meters.
- **Structural materials:** Although not detailed in the summary, they are often used aerospace **aluminum with titanium reinforcements and carbon fiber composites** to minimize weight and maintain structural strength.

Thermal Protection System

- **Type:** Heat shield type C-C (**Carbon-Carbon**).
 - **Material base:** Composed of carbon **fiber reinforced carbon**, highly resistant to extreme temperatures, used in applications such as spacecraft leading edges.
 - **Key properties:**
 - Low thermal conductivity.
 - Structural stability to more than 1,400°C.
 - High emissivity and wear resistance.
 - **Maximum diameter of the TPS:** 2.3 meters.
- **Purpose:** Absorb and deflect concentrated solar flux at perihelion (~9.86 solar radii) and protect instruments.

Heat release in nozzle: recombination of dissociated molecules (e.g., $H + H = H_2$) and exothermic reactions due to changes in equilibrium composition cause internal heating of the expanding gases. Particulates also release heat to the gas.

Nozzle shape and size: can use straight cones, bell-shaped, or other nozzle contours; bell shapes may yield slightly lower losses. Apply corrections for divergence losses and nonuniformity of the velocity profile.

Gas properties: the governing relationships for gas behavior apply to both nozzle and chamber conditions. As gases cool during expansion, some species may condense.

Nozzle exit conditions: will depend on prior assumptions regarding chemical equilibrium, nozzle expansion, and nozzle contour. Assume no jet separation. Determine the velocity and pressure profiles at the nozzle exit plane. If pressure is not uniform across the section, cross flow will occur.

Calculate specific impulse: can be determined for varying altitudes, pressure ratios, mixture ratios, and nozzle area ratios. Heat release in the subsonic portion of the nozzle increases exit velocity, while heating in the supersonic section can raise exit temperature but lower exit Mach number. Must assume or define a specific nozzle configuration. Bell contours can be calculated using the method of characteristics. Use Eq. 3-34 for divergence losses in conical nozzles. Most analysis tools are one- or two-dimensional.

Asymmetrical nonround nozzles may require three-dimensional analysis. Use perfect gas laws, or real gas properties if some species approach condensation.

Need to know the nozzle area ratio or pressure ratio. For quasi-one-dimensional and uniform nozzle flow, refer to Eqs. 3-25 and 3-26. If velocity (v_2) is not constant across the exit area, determine the effective average values of v_2 and p_2 , then calculate the temperature (T), density (ρ), and other profiles. For

nonuniform velocity profiles, an iterative approach is required. Gas conditions (T, p, etc.) can be calculated at any point within the nozzle.

When the **fuel-to-oxidizer ratio** is rich (more hydrogen than needed for complete combustion), the combustion temperature is lower, and the amounts of certain products like **atomic oxygen (O)**, **atomic hydrogen (H)**, **hydroxyl (OH)**, and **unreacted oxygen (O₂)** become **very small**.

In such cases, we can **neglect** these components to simplify the analysis and focus only on the major species, like water vapor and unburned hydrogen.

Solving the Reaction

The problem typically involves finding the **combustion temperature** and the amounts of each product species. However, only a limited number of equations are available — for example:

- One from energy balance (heat released = heat absorbed by gases)
- Two from mass balance (hydrogen and oxygen)

In a simplified view, the **left side** of a chemical reaction shows the initial state (hydrogen and oxygen), and the **right side** shows the final state, which includes water and other species formed as a result of the combustion.

Not all hydrogen and oxygen molecules react completely — some may remain **unreacted**, depending on the mixture and conditions.

At a given temperature and pressure, the composition of the reaction products will reach a state of **chemical equilibrium**, where the concentrations of all species stay constant.

Combustion of Hydrogen with Oxygen

The **combustion of hydrogen with oxygen** is often used as a classic example in propulsion and thermodynamics studies. This reaction can produce **six possible gaseous products**:

- Water vapor (H₂O)
- Molecular hydrogen (H₂)
- Molecular oxygen (O₂)
- Hydroxyl radical (OH)
- Atomic oxygen (O)

- Atomic hydrogen (H)

Although **ozone (O₃)** and **hydrogen peroxide (H₂O₂)** could theoretically form as byproducts, they are **unstable at high temperatures** and are typically ignored in combustion analysis.

General form of mass balance:

The **mass of any given element must** be the same before and after the reaction. The number of kg-mol **of a given element per kilogram of** reactants and products must be equal, that is, their difference must be zero.

For each atomic species, such as H or O in Equation (5–20):

$$\left[\sum_{j=1}^m a_{ij} n_j \right]_{\text{productos}} - \left[\sum_{j=1}^r a_{ij} n_j \right]_{\text{reactantes}} = 0$$

The **combustion of hydrogen with oxygen is** used below as an example.

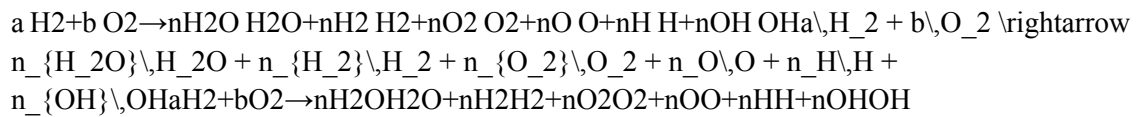
It can produce six **possible products**:

- Water (H₂O)
- Hydrogen (H₂)
- Oxygen (O₂)
- Hydroxyl (OH)
- Atomic oxygen (O)
- Atomic hydrogen (H)

Here, all reactants and products are gaseous. Theoretically, there could be two additional products:

- Ozone (O₃)
- Hydrogen peroxide (H₂O₂)

Mass balance in chemical notation:



The left side shows the conditions before **the reaction** and the right side shows the condition after **the reaction**.

Given that **H₂** and **O₂** are found on both sides, this means that **Not all of these species are consumed**, and a portion of them, i.e. $n\text{H}_2n_{\{\text{H}_2\}}n\text{H}_2$ and $n\text{O}_2n_{\{\text{O}_2\}}n\text{O}_2$, will remain unreacted.

At any particular temperature and pressure, the molar concentrations on the right-hand side will remain fixed when the chemical **equilibrium**.

Instructions:

Sample signals from significant sensors (e.g., chamber pressure, gas and hardware temperatures, tank pressure, valve position, etc.) at frequent intervals, say once, 10, 100, or 1,000 times per second. For slowly changing parameters (such as control box temperature), sampling every second or every 5 seconds may be sufficient, but the chamber pressure would be sampled at a high frequency.

Keep a log of all significant signals received and all signals generated by the computer and sent as commands or information. Old logs have sometimes been very important.

Control and verify the engine startup steps and sequence. Figure 11-3 and Table 11-4 list the typical steps to be taken, but they do not list the measured parameters that will confirm that the commanded step was implemented. For example, if the igniter is activated, a signal change from a well-located temperature sensor or radiation sensor could verify that ignition actually occurred.

Control engine shutdown. For each of the steps

there must often be a detection of a change in pressure or other parameter to verify that the commanded shutdown step was taken. An emergency shutdown may be ordered by the controller during development testing when it detects certain types of faults that allow the engine to be shut down safely before a dramatic failure. This emergency shutdown procedure must be performed quickly and safely and may be different from the normal shutdown to avoid creating a new hazardous condition.

Limit the duration of full-power operation. For example, the shutdown should be initiated just before the vehicle reaches the desired mission speed.

Safety monitoring and control. Detect combustion instability, over temperatures in pre-combustion chambers, gas generators, or TP bearings, violent vibrations in TP, TP overspeed, or other parameters known to cause rapid and drastic component failures that can quickly lead to engine failure. Typically, more than one sensor signal will indicate such a failure. If detected by multiple sensors, the computer can identify it as a potential failure with a known (and pre-programmed) in-flight remedy; it can then

automatically order corrective action or a safe shutdown. This primarily applies to development engines during ground testing.

Analyze key sensor signals to detect deviations from rated performance before, during, and after engine operation. Determine whether the detected quantities are outside expected limits. If appropriate and feasible, and if more than one sensor indicates a possible out-of-range value, and if the cause and remedy can be predicted (pre-programmed), then the computer can automatically initiate compensatory action. Parts or combinations of items 6 and 7 have been called engine health monitoring systems. They are discussed in Section 11.5.

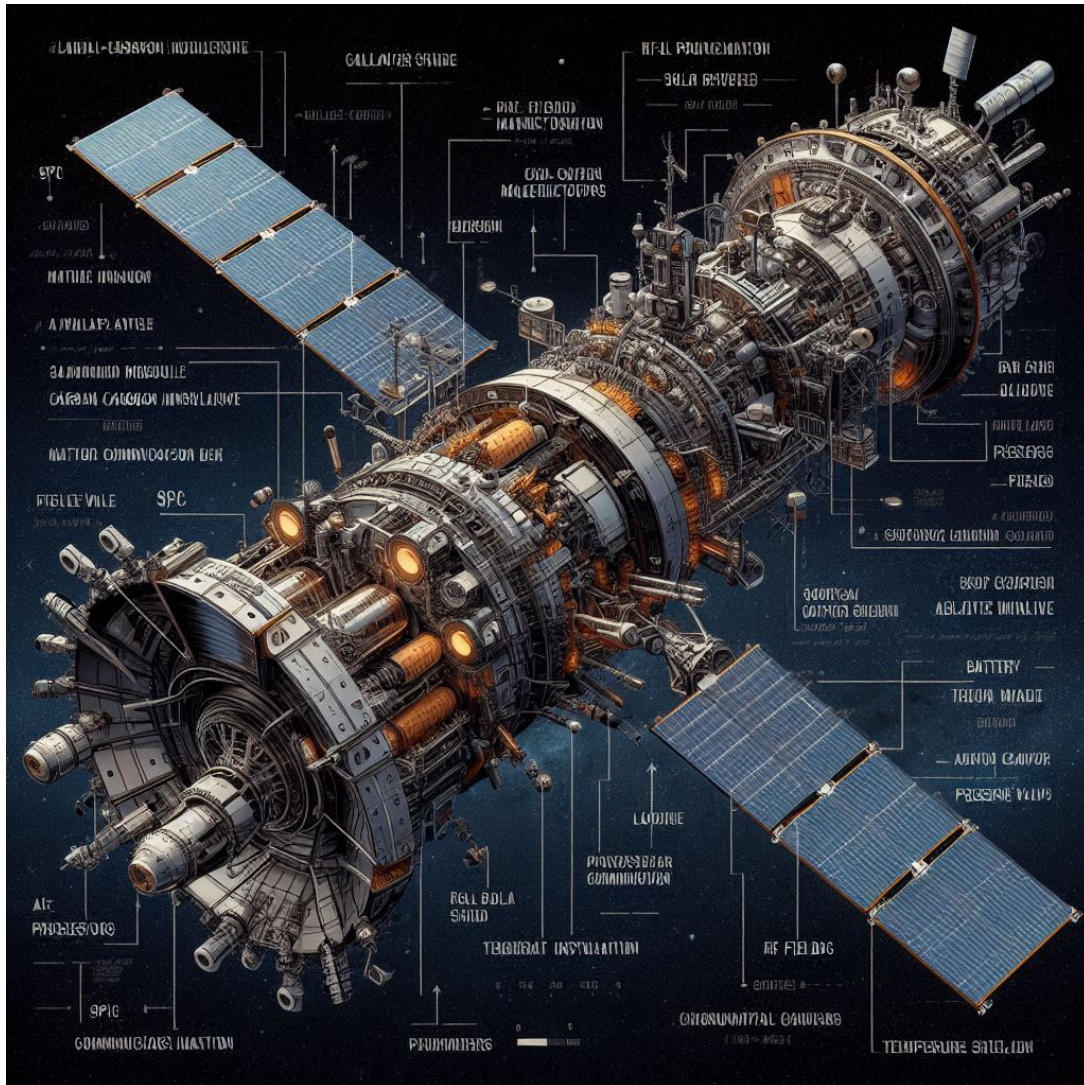
Control propellant tank pressurization. The tank pressure must be within an allowable range during engine operation and also during a glide flight period prior to a restart. Detection of tank relief valve activation confirms overpressure. The computer can automatically command the pressurizing gas flow to be stopped or reduced.

Perform automatic closed-loop control of thrust and propellant utilization (described above).

Transmit signals to the craft's telemetry system, which can then send them to a ground station, providing information on engine status, especially during experimental or initial flights.

Computer and software self-test.

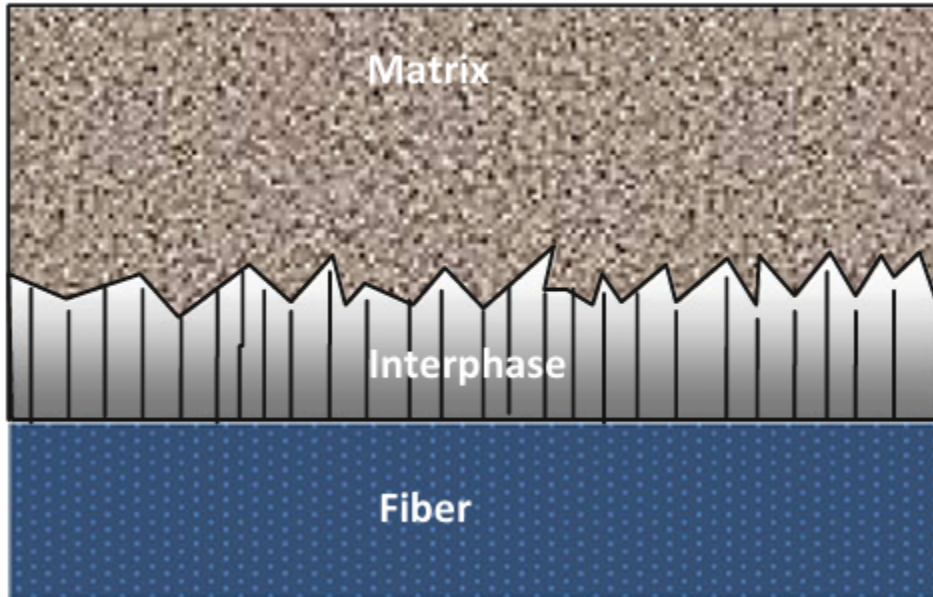
Technical blueprint of a futuristic spacecraft in orbit, labeled components including carbon-carbon heat shield, propulsion system, solar panels, propellant tanks, exoskeleton structure, realistic aerospace systems, spacecraft in space, thermal radiators, high-gain antennas, all drawn in blueprint style with fine white lines on dark blue background, detailed technical schematic, minimalist, realistic layout for aerospace engineering purposes.



A detailed spacecraft technical cutaway diagram in space, labeled blueprint-style, showcasing realistic components based on Parker Solar Probe: radiators (CSPR), louvers (10/20-blade), multilayer insulation, AI command module, solar arrays, ion propulsion, RF communication deck, carbon-carbon ablative shields, temperature sensors, pressure valves, battery with 7-blade louver, and scientific instruments (SPAN-B, SPC, FIELDS). Include labeled boom-mounted magnetometers, data mining AI modules, realistic wiring and structure, deep space backdrop, Earth visible, NASA-like schematic with clean lines and technical annotations. Emphasize futuristic but scientifically plausible engineering.

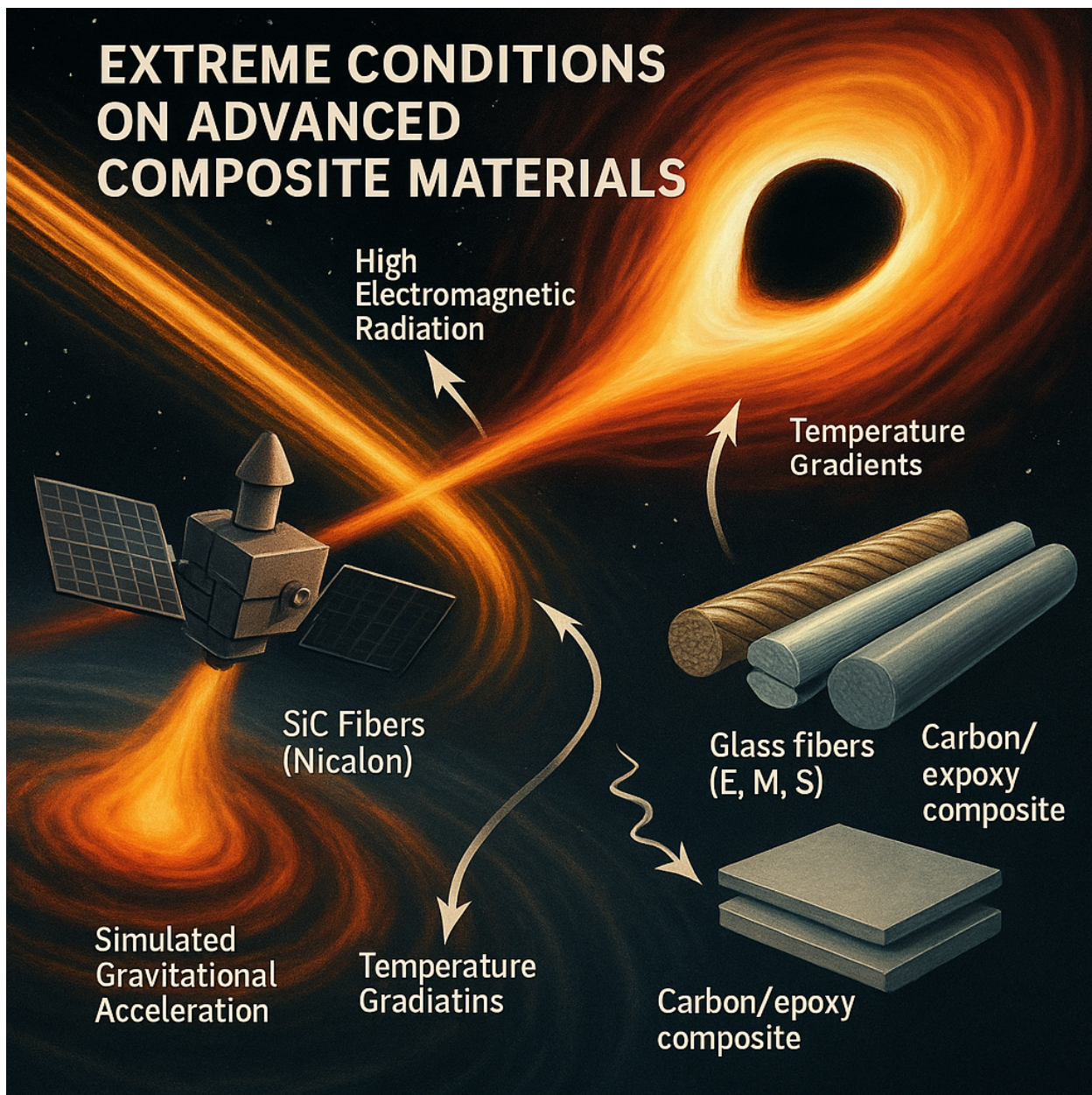
Interfaces of Fiber-Reinforced Resin Matrices FMLs make up only a small part of the advanced composites family; the largest member is fiber-reinforced polymer composites. In fact, the Al plate surfaces and interfaces generated in the compositing of metal and resin described above did not include the fiber surface or the interface between fiber and resin. The main reason for this is because surface treatment of fibers is normally carried out to match the resin matrix in the fiber suppliers before composite manufacture, and usually the compatibility between fiber and resin can meet the service requirements for composites. In other words, commercial fibers have already been coated, so they can be defined according to the resin coating rather than the fiber surface itself. The sizing and finishing of

commercial fibers are diverse and can be organic- or water-based, including diluted resin, curing agent, surface lubricant, antistatic agent, pH-adjusting agent and emulsions.



Fibers are usually coated with multiple layers to obtain combined performance. The main functions of sizing and finishing are to protect the structure and surface conditions of the fresh fibers to obtain good interface adhesion between the fiber and resin (coupling effect) and to increase their anti-friction and antistatic properties. Fiber surface-treating agents and their applications are core techniques in fiber production. Because the suppliers must satisfy various customers, the surface coatings for commercial fibers must be general purpose.

EXTREME CONDITIONS ON ADVANCED COMPOSITE MATERIALS



As airplane fuselage materials, two critical characteristics of carbon fiber laminates, their impact damage resistance (tolerance) and glass transition temperature (T_g , or thermal-wet service temperature), are determined by the resin matrix. In the aerospace industry, the impact damage resistance is expressed as compression strength after impact (CAI) and is usually used to classify resin toughness and generation.

The first generation of aerospace composites (Composites) was simply laminates (2–2 composition) composed of resin (Ares Phase 0 3) and fibers (Reinforcement 2 2 can be expressed as Are In Phase 0 3 β B reinforcement 2 2 $\frac{1}{4}$ C reinforcement).

Based on δ A1P resin 33 β δ A2 β B2 2 Reinforce 2 2 $\frac{1}{4}$ Ccomposite 2 2 ,

Composite materials in the aerospace industry: The combined product prepared from the second reactive constituent (A2) and carbon fiber fabric (B2–2). The first reactive constituent (A1) with low viscosity was added by injection at low temperature until fibers were fully immersed and impregnated and then heated to achieve further chemical reaction. During the chemical reaction, resin parts A2 and A1 adhered to fiber fabric B2–2 were dissolved and infused to form a uniform phase, increasing the immersing effect. The final dried fabric was fully impregnated with resin.

Material example: Epoxy resin composites(RTM) Service temperature 75°C,3266ES CAI 300MPa Performance Equivalent to or higher than that of CYCOM 823 RTM.

Fiber Reinforcement:

Glass fibers are usually drawn from a molten mixture of quartz sand, limestone, dolomite and paraffin, as well as a certain fraction of soda and boric acid [4]. To facilitate the process or to achieve the desired performance, an appropriate fraction of TiO₂, ZrO₂ or Al₂O₃ is also incorporated. The components and the drawing process greatly affect the performance of the final fibers. Glass fibers are non-combustible and do not decompose, and they are characterized by good chemical stability, good heat resistance, high tensile strength, high electrical insulation, low tensile strain, low insulation and a low coefficient of thermal expansion. They were the first fibers to be used for the preparation of polymer matrix composites. They are commonly known to be low-cost reinforcements for fiberglass-reinforced plastics (FRP) [5]. The diameters of the glass fibers vary from 5 to 20 lm, and a finer fiber diameter generally results in better performance. The types and specifications of commercially available glass fibers are mainly as follows: A-glass fiber, containing high alkali metal oxides; C-glass fiber, resistant to chemical attack; D-glass fiber, with a high dielectric property; E-glass fiber, with high electric insulation; M-glass fiber, with a high Young's modulus; S-glass fiber, with a high tensile strength; AR-glass fiber, alkaline resistant and suitable for reinforcing cement matrix composites.

E-Glass Fibers E-glass fibers, also referred to as non-alkali glass fibers, were the first fiber species used for electronic insulation belts. They are a kind of Ca-Al-B-Si glass fiber with a total alkali content less than 0.8 wt%, which ensures their excellent corrosion resistance and high conductivity resistance. As a favored insulation material, they have been processed into electromagnetic wires, impregnation materials, mica products, laminated products and polymer matrix composite products. The insulation grade of these products varies from B, F and H to C, which enables their widespread use in the electric and electronic fields. They are also the most common fiber reinforcements for polymer matrix composites.

M-Glass Fibers M-glass fibers, also referred to as high-modulus glass fibers, generally have a higher modulus than common glass fibers. Their specific modulus is much higher than that of steel because their density is about two-thirds lower. Improving the modulus of glass fibers allows their use in structural composites, which results in better performance. For SiO₂-Al₂O₃-MgO glass fibers, oxides such as BeO, Y₂O₃, ZrO₂, TiO₂ and CeO₂ are usually incorporated to increase their Young's modulus. However, highly toxic BeO and expensive Y₂O₃ have not been industrially used even though they are particularly effective in increasing moduli. Chinese type "M2" glass fibers with a Young's modulus of about 95 GPa have been produced, and they contain CeO₂, TiO₂ and ZrO₂.

High Silica Glass Fibers High silica glass fibers contain about 96–99 wt% SiO₂ as well as small amounts of B₂O₃, Na₂O and Al₂O₃. For the preparation of SiO₂–B₂O₃–Na₂O system glass fibers, raw materials were molten and drawn into fiber products, phase separated at 500–600 °C and then soaked in hydrochloric acid at a certain temperature. B₂O₃ and Na₂O were leached, and a porous SiO₂ skeleton was left; the skeleton was then sintered at 700–900 °C with the SiO₂ content increasing to more than 96 wt%. The high silica glass fibers have fiber diameters of 4–10 lm, a density of 2.20 g/cm³, a tensile strength of 1.50 GPa and a Young's modulus of 73 GPa. The main characteristics of these products are high-temperature stability, shape stability, thermal shock resistance and chemical stability, which enable their use as a high-temperature ablation reinforcement.

a new type of glass fiber, hollow glass fibers have features such as lightness, high stiffness, low dielectric constants and low thermal conductivity. Their main technical indexes are hollow percentage and hollow degree. The hollow percentage refers to the ratio of the number of hollow filaments versus the total number of filaments and is expressed as a percentage; the hollow degree refers to the ratio of the inner diameter versus the outer diameter of the hollow fibers, often expressed as a K value.

Hollow fibers are generally prepared from E-glass. Their tensile strength increases when the K value increases from zero to 0.8 and decreases when the K value increases more than this. For general industrially produced hollow glass fibers, K = 0.5 – 0.7. They are characterized by low thermal conductivity and low dielectric constant, as listed in Table 2.7. Composites made from hollow glass fibers can be used in the aviation industry and in underwater facilities such as radomes, deep water containers and high pressure containers. Additionally, hollow glass fibers with metal coatings of zinc or aluminum can be used as electronic-interference materials. Because of their excellent lightness, reliability, capacity and response time, they can float in air over long periods and proliferate over a large area while having good interference effects. These antistatic and electromagnetic shielding fields.

Radiation-Resistant Insulating Fibers These fibers are composed of SiO₂, Al₂O₃, CaO and MgO and characterized by a small thermal neutron capture area, high insulation resistance, excellent mechanical properties and better water resistance than E-glass fibers. Their insulation resistance is highly stable under high doses of c-rays or strong neutron irradiation. The fibers can thus be used at high temperatures and under strong irradiation environments. For example, they can be used as main insulation materials in high-temperature cables or radiation-resistant cables in nuclear reactors. They are also insulation materials that can be used for high-temperature wires and are important reinforcements for polymer matrix composites.

Carbon Fibers Fibrous carbons include continuous carbon (graphite) fibers, carbon whiskers and the recently developed carbon nanotubes, and these are new types of nonmetallic materials [3]. Among them, carbon fibers are a kind of polycrystalline fiber with incompletely crystallized graphite arranged along the fiber axial [6].

Carbon fibers are manufactured from carbon precursors followed by spinning into fiber form (spinning step), cross-linking using proper agents (stabilization step), and heating up to 1200–3000 °C under inert gas to remove non-carbon elements (carbonation step) [6–21]. As the most successful commercialized

carbon products in the last 40 years, carbon fibers have developed into one of the most important modern industrial materials. They are mainly used as reinforcements for polymer matrices, ceramic matrixes and carbon matrix composites. At present, most countries regard high-performance carbon fibers as important engineering materials for the twenty-first century [6, 7]. Based on their mechanical properties, carbon fibers can be classified into the following categories: high-tenacity type (HT), ultra-high-tenacity type (UHT), high-modulus type (HM) and ultra-high-modulus type (UHM). Their corresponding mechanical property ranges are listed in Table 2.8. Based on the type of carbon precursor, carbon fibers can be classified as poly acrylonitrile (PAN)-based carbon fibers, pitch-based carbon fibers and rayon (viscose filament)-based carbon fibers, whose typical species and major mechanical properties are listed in Tables 2.9, 2.10 and 2.11. From the above tables, the most representative manufacturer is the Toray Company, whose high-performance carbon fibers are second to none in terms of production and performance. Additionally, their fiber varieties tend to be serialized [8–12]. As functional reinforcements, in addition to high specific strength and high specific modulus [10], carbon fibers also have excellent properties like high-temperature stability, chemical corrosion resistance, heat impact resistance, electrical conductivity, thermal conductivity, anti-friction properties, anti-radiation properties, damping, shock absorption, noise reduction and availability. Carbon fiber-reinforced composites have been widely used in the aerospace, defense and other military fields, as well as in advanced sporting goods, medical equipment, the auto industry and in other civilian areas. Their fields of application and their characteristics.

```

fiber_type = "PAN-CF"
manufacturer = "Amoco"
brand = "T-50"
diameter_um = 6.5
density_g_cm3 = 1.81
tensile_strength_GPa = 2.90
youngs_modulus_GPa = 300
tensile_strain_pct = 0.7
compressive_strength_GPa = "1.61-4.09"
note = "C"

```

```

fiber_type = "PAN-CF"
manufacturer = "Amoco"
brand = "T-40"
diameter_um = 5.1
density_g_cm3 = 1.81
tensile_strength_GPa = 5.65
youngs_modulus_GPa = 290
tensile_strain_pct = 1.8
compressive_strength_GPa = "1.88-2.7"
note = "C"

```

```

fiber_type = "PAN-CF"

```

```
manufacturer = "Amoco"
brand = "T-650/35"
diameter_um = 6.8
density_g_cm3 = 1.77
tensile_strength_GPa = 4.55
youngs_modulus_GPa = 241
tensile_strain_pct = 1.8
compressive_strength_GPa = 0.8
note = "C"
```

```
fiber_type = "PAN-CF"
manufacturer = "Amoco"
brand = "T-300"
diameter_um = 7.0
density_g_cm3 = 1.76
tensile_strength_GPa = 3.45
youngs_modulus_GPa = 231
tensile_strain_pct = 1.4
compressive_strength_GPa = "2.8-2.88"
note = "C"
```

```
fiber_type = "PAN-CF"
manufacturer = "Amoco"
brand = "T-300"
diameter_um = 7.0
density_g_cm3 = 1.76
tensile_strength_GPa = 3.45
youngs_modulus_GPa = 231
tensile_strain_pct = 1.4
compressive_strength_GPa = "2.8-2.88"
note = "C"
```

```
fiber_type = "PAN-CF"
manufacturer = "Amoco"
brand = "T-300"
diameter_um = 7.0
density_g_cm3 = 1.76
tensile_strength_GPa = 3.45
youngs_modulus_GPa = 231
tensile_strain_pct = 1.4
compressive_strength_GPa = "2.8-2.88"
note = "C"
```

Carbon fibre properties:

```
fiber_type = "PAN-CF"
manufacturer = "Hercules"
brand = "Magnamite-AS4"
shear_modulus_GPa = 17.0
damping_factor = 1.10

2)
fiber_type = "PAN-CF"
manufacturer = "Toray"
brand = "Torayca-M30"
damping_factor = 1.42
horizontal_compressive_modulus_GPa = 3.2

3)
fiber_type = "PAN-CF"
manufacturer = "Toray"
brand = "Torayca-T40"
shear_modulus_GPa = 14.0
damping_factor = 2.00
horizontal_compressive_modulus_GPa = 17.0
horizontal_fracture_strain_pct = 1.96

4)
fiber_type = "PAN-CF"
manufacturer = "Toray"
brand = "Torayca-T40J"
damping_factor = 3.52
horizontal_compressive_modulus_GPa = 4.0
horizontal_compressive_strength_MPa = 17.5
horizontal_fracture_strain_pct = 1.98

5)
fiber_type = "PAN-CF"
manufacturer = "Toray"
brand = "Torayca-T50"
shear_modulus_GPa = 14.0
damping_factor = 1.50
horizontal_compressive_modulus_GPa = 15.0
horizontal_fracture_strain_pct = 1.36

6)
fiber_type = "PAN-CF"
manufacturer = "Toray"
brand = "Torayca-T300"
horizontal_compressive_strength_MPa = 556
horizontal_fracture_strain_pct = 26
shear_modulus_GPa = 15.0
```

```
damping_factor = 1.30
horizontal_compressive_modulus_GPa = 3.21
```

Pitch-CF Type

```
8) fiber_type = "Pitch-CF"
manufacturer = "Amoco"
brand = "Thornel-P25"
horizontal_compressive_strength_MPa = 600

9) fiber_type = "Pitch-CF"
manufacturer = "Amoco"
brand = "Thornel-P55S"
horizontal_compressive_strength_MPa = 300
shear_modulus_GPa = 6.6
damping_factor = 0.85
horizontal_compressive_modulus_GPa = 7.0

10) fiber_type = "Pitch-CF"
manufacturer = "Amoco"
brand = "Thornel-P75S"
horizontal_compressive_strength_MPa = 200
shear_modulus_GPa = 8.0
damping_factor = 0.85
horizontal_compressive_modulus_GPa = 9.0
damping_factor_2 = 0.88

11) fiber_type = "Pitch-CF"
manufacturer = "Amoco"
brand = "Thornel-P100"
horizontal_compressive_strength_MPa = 130
shear_modulus_GPa = 4.7
damping_factor = 1.00
horizontal_compressive_modulus_GPa = 5.0
damping_factor_2 = 1.04
```

DuPont de Nemours

```
1) fiber_type = "Pitch-CF"
manufacturer = "DuPont de Nemours"
brand = "FiberG-E35"
horizontal_compressive_strength_MPa = 80
```

```

shear_modulus_GPa = 8.0
damping_factor = 0.70
horizontal_compressive_modulus_GPa = 8.5
damping_factor_2 = 0.73

2) brand = "FiberG-E75"
shear_modulus_GPa = 5.7
damping_factor = 1.00
horizontal_compressive_modulus_GPa = 6.0
damping_factor_2 = 1.01

3) brand = "FiberG-E105"
shear_modulus_GPa = 5.0
damping_factor = 1.00
horizontal_compressive_modulus_GPa = 5.5
damping_factor_2 = 1.04

```

Mitsubishi / Nippon Steel

```

fiber_type = "Pitch-CF"
manufacturer = "Mitsubishi NipponSteel"
brand = "NT-20"
horizontal_compressive_strength_MPa = 160
horizontal_fracture_strain_pct = 8

brand = "NT-40"
horizontal_compressive_strength_MPa = 94.3
horizontal_fracture_strain_pct = 10

brand = "NT-60"
horizontal_compressive_strength_MPa = 54.9
horizontal_fracture_strain_pct = 5

```

PAN-based carbon fibers are characterized by the following features: ① good weaving capability; ② low density, 1.7–2.1 g/cm³; ③ high modulus, 200–700 GPa; ④ high strength, 2–7 GPa; ⑤ fatigue resistant; ⑥ self-lubricating and wear resistant; ⑦ energy absorbing and impact resistant; ⑧ low coefficient of thermal expansion, 0–1.1 10–6 K⁻¹; ⑨ good thermal conductivity without heat accumulation; ⑩ good electrical conductivity, 15–5000 S/m, and non-magnetic; good X-ray penetration and good biological compatibility. Toray is the most comprehensive company in terms of PAN-based carbon fiber production, and their fiber specifications and performances are listed in Table 2.14[8]. The performance of carbon fibers increases from T300 to T1000G and from M30S to M60 J.

Ceramic Fibers:

Advanced ceramics mainly refer to nonmetallic oxides, quasi-metal oxides, carbides, nitrides, alumina, aluminum nitride and carbon, etc. Their raw materials are generally high purity, ultra-fine synthetic inorganic compounds. Their common characteristics are high-temperature stability, oxidation resistance, erosion resistance, corrosion resistance, wear resistance, high hardness and a low creep rate as well as coupling features related to their light, electrical, magnetic, acoustic and thermal properties. They are mainly used in high-tech and military technical areas that require high-temperature stability, corrosion resistance and wear resistance, etc. Examples might be mechanical seals, ceramic bearings, ball valves, ceramic cylinders and cutting tools. With the development of materials science and engineering, advanced ceramic materials have developed from polycrystalline bulk materials to low-dimensional materials such as fibers or whiskers.

Rayon-Based Carbon Fibers a-Cellulose can be extracted from cellulose raw materials such as wood, cotton seed cashmere and bagasse. When they are purified with soda or carbon disulfide, dissolved in dilute NaOH, wet-spun and post-processed, viscose fibers are obtained. Carbon fibers can be obtained after oxidation in air below 300 °C and carbonization in inert atmosphere above 800 °C. If graphitized in argon above 2500 °C, their crystallinity, thermal conductivity, anti-oxidation, lubrication and heat capacity increase greatly and graphite fibers are obtained with a carbon content of more than 99%.

fibers play an irreplaceable role in thermal insulation-resistant and ablative materials, in reinforcement materials as well as in promising biological engineering materials because of their excellent biocompatibility. Brand names and properties of rayon-based carbon fiber products.

Rayon-based carbon fibers are mainly used as large area ablation shielding materials for aircraft brakes, car brakes, radioisotope boxes, solid-fuel engine nozzles, reentry vehicles, rocket and missile noses or heads. They can also be used to reinforce polymer composites with applications in corrosion-resistant pumps, laminas, pipes, containers and conductive wires, heating bodies, sealing materials, catalyst supports and medical absorption materials, and colloidal materials in addition to medical bandages and anti-chemical clothes.

Variables & tensile strength:

```
manufacturer = "UCC"
brand = "Thornel-25"
tensile_strength_GPa = 1.260
youngs_modulus_GPa = 175
density_g_per_cm3 = 1.40 # to 1.45
```

```

manufacturer = "UCC"
brand = "Thornel-40"
tensile_strength_GPa = 1.750
youngs_modulus_GPa = 280
density_g_per_cm3 = 1.56

manufacturer = "UCC"
brand = "Thornel-50"
tensile_strength_GPa = 1.995
youngs_modulus_GPa = 350
density_g_per_cm3 = 1.60

manufacturer = "UCC"
brand = "Thornel-100"
tensile_strength_GPa = 3.500
youngs_modulus_GPa = 700
density_g_per_cm3 = 1.79

manufacturer = "HITCO"
brand = "HMG-20"
tensile_strength_GPa = (1.120, 2.100)
youngs_modulus_GPa = (154, 210)
density_g_per_cm3 = 1.5

manufacturer = "HITCO"
brand = "HMG-40"
tensile_strength_GPa = (1.400, 1.645)
youngs_modulus_GPa = (245, 350)
density_g_per_cm3 = 1.7

manufacturer = "HITCO"
brand = "HMG-50"
tensile_strength_GPa = (2.100, 2.205)
youngs_modulus_GPa = (350, 427)
density_g_per_cm3 = 1.8

```

These materials should have excellent chemical and thermal mechanical stability at 1500°C.

Some oxide ceramics like quartz and Al₂O₃ can be melt-spun into ceramic fibers using high purity or controlled purity and composition ceramic materials, but most ceramics cannot be directly spun into ceramic fibers because of their high melting points. The general approach is to synthesize pre-ceramic precursors, which could be either inorganic precursors or organic polymer precursors. The precursors can be easily spun into green fibers and then be transformed into ceramic fibers after firing and sintering at

high temperatures. Like organic fibers, ceramic fibers have high strength, high modulus, fine diameters and good weaving performance; however, ceramic fibers also have high-temperature stability, oxidation resistance and high hardness. Therefore, ceramic fibers are believed to be important reinforcements for advanced polymers, metals and ceramic matrix composites.

Alumina Fibers The main phase of alumina fibers is a-Al₂O₃, and small amounts of SiO₂, B₂O₃, ZrO₂, MgO, etc. are also present. These fibers have excellent high-temperature oxidation resistance and high-temperature stability as high as 1400 °C. They have been given much attention recently. As a typical example, the 3M Company in the USA produced a new Al₂O₃ fiber using iron oxide for grain refinement. The tensile strength and elasticity modulus of this fiber are as high as 3.2 and 370 GPa, respectively (Nextel610). In addition, Nextel610 has a low thermal conductivity, unique electrochemical properties and corrosion resistance properties:

```
brand = "FP"
manufacturer = "DuPont"
diameter_um = (15, 20)
composition = {"Al2O3": 99}
tensile_strength_GPa = (1.4, 2.1)
youngs_modulus_GPa = (350, 390)
tensile_strain_pct = 0.29
density_gcm3 = 3.95
working_temp_C = (1000, 1100)

brand = "PRO"
manufacturer = "DuPont"
diameter_um = (15, 25)
composition = {"Al2O3": 80, "ZrO2": 20}
tensile_strength_GPa = (2.2, 2.4)
youngs_modulus_GPa = (385, 420)
tensile_strain_pct = (0.40, None) # hasta 1400 °C

brand = "Altel"
manufacturer = "Sumitomo"
diameter_um = (9, 17)
composition = {"Al2O3": 75, "SiO2": 25}
tensile_strength_GPa = (1.8, 2.6)
youngs_modulus_GPa = (210, 250)
tensile_strain_pct = 0.80
density_gcm3 = (3.2, 3.3)
working_temp_C = 1250
```

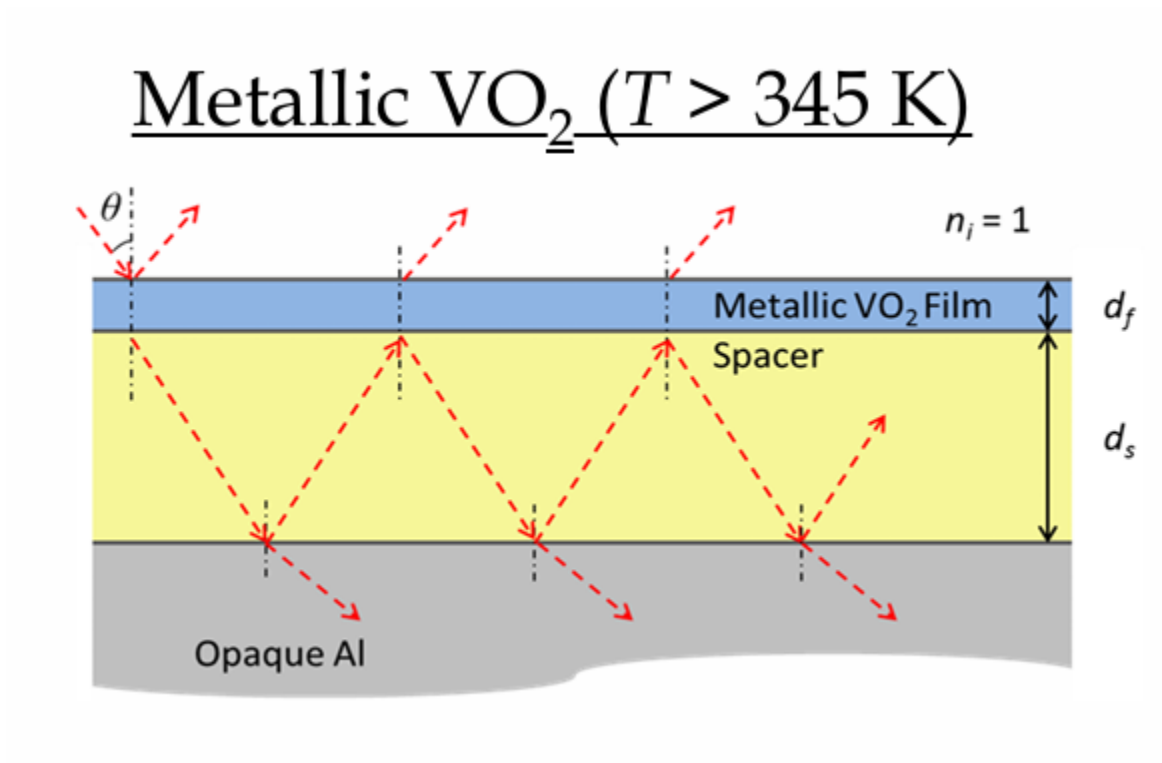
The mechanical properties and to improve the hardness and wear resistance of the matrixes, alumina fibers have low density, good insulation, low thermal capacity, are effective energy savers, and have a low

coefficient of thermal expansion. Therefore, alumina fiber-reinforced aluminum matrix composites have been applied to the production of car pistons, connecting rods, brake parts, gas compressor rotating blades and helicopter transmission devices. At high temperatures, the Fabry-Perot resonance cavity is formed, leading to an emission enhancement near resonance wavelength of $\lambda = 10 \mu\text{m}$

($T > 345 \text{ K}$)

Insulating VO₂

At low temperatures, the structure becomes highly reflective due to the high IR transmittance of the VO₂ and spacer material



Variables:

ϵ_∞ = High frequency dielectric constant

S_j = Phonon strength

ω_j = Phonon frequency

ω_p = Plasma frequency

ω_c = Collision frequency

q = Depolarization factor

f = Filling Fraction

γ_j = Damping Coefficient

Fiber reinforcement:

```

fiber = {
    "brand": "NL202",
    "manufacturer": "Nippon Carbon",
    "composition": {"Si": 57, "C": 31, "O": 12},
    "density_gcm3": 2.55,
    "diameter_um": 14,
    "tensile_strength_GPa": 3.0,
    "youngs_modulus_GPa": 220,
    "status": "C"
}

```

(C core) fibers were produced with better performance and lower cost. Subsequently, from 1981 to 1984, SiC (C core) fibers were successfully commercialized by AVCO. Recently, the US company Textron (formerly AVCO Corporation) was allowed to produce a series of SCS-2, SCS-6 and SCS-8 SiC (C core) fibers. British company BP bought the original German technology for the production of SiC (W core) fibers. It produced a series of fibers referred to as SM1040, SM1140 and SM1240 with different surface coatings. These fibers were applied, respectively, to reinforce polymers, aluminum, titanium, intermetallic compounds and ceramic matrixes.



- VO₂ Thickness:

$$d_f = 25 \text{ nm}$$

- Spacer Thickness:

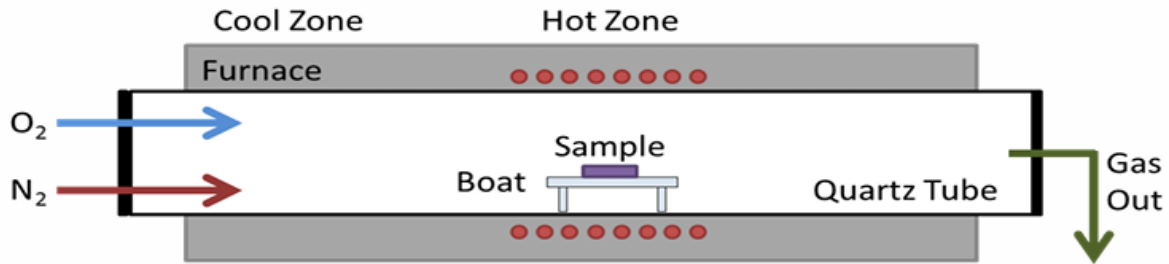
$$d_s = \lambda_{\text{peak}} / 4n \approx 730 \text{ nm}$$

where $\lambda_{\text{peak}} = 10 \mu\text{m}$

$$n = 3.4$$

What furnace conditions do we need?

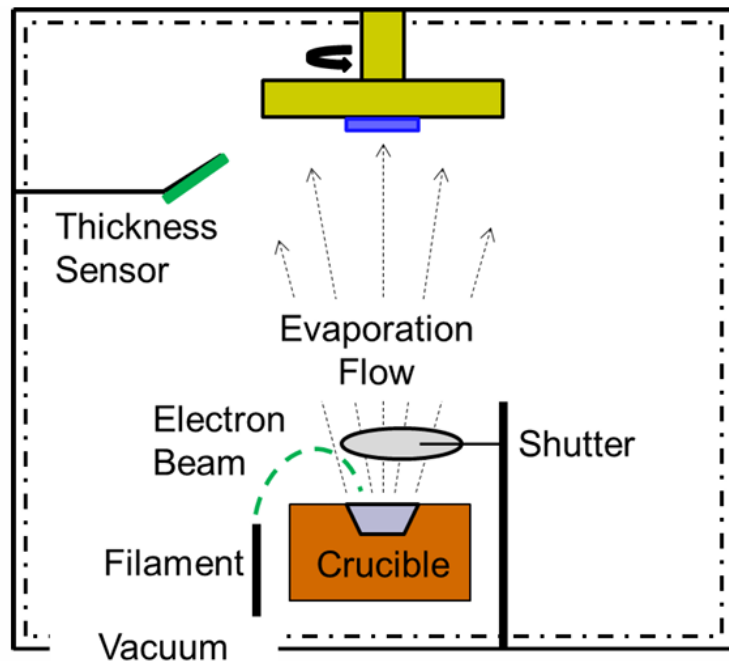
- Temperature
- Furnace Time
- O₂ flow rate
- N₂ flow rate Conducted series of parametric studies to determine optimal conditions



```

fiber = {
    "brand": "Hi-Nicalon",
    "manufacturer": "Nippon Carbon",
    "composition": {"Si": 62, "C": 32, "O": 0.5},
    "density_gcm3": 2.74,
    "diameter_um": 14,
    "tensile_strength_GPa": 2.8,
    "youngs_modulus_GPa": 270,
    "status": "C"
}

```

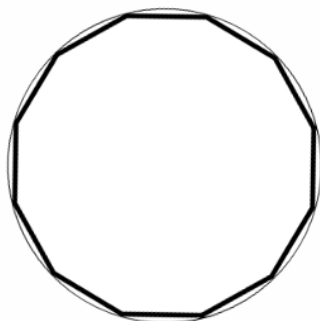


Pre-ceramic Polymer-Derived (PPD) SiC Fibers The precursor approach of transferring organic materials into inorganic materials by high-temperature treatment under oxygen-free atmospheres has been used since ancient times. Similar to the method to obtain carbon fibers wherein PAN or other organic fibers are

carbonized in an inert atmosphere at high temperatures, this kind of precursor method has been applied to the commercial production of ceramic fibers. The process includes four steps:

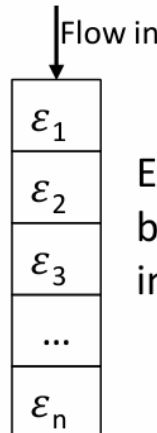
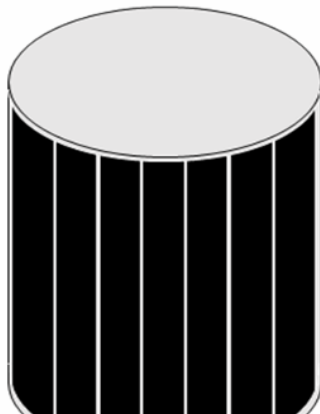
- 1 synthesis of preceramic polymers (pre cursors);
- 2 melt spinning of polymers into green fibers;
- 3 curing of green fibers by oxidation or EB radiation, and
- 4 pyrolysis of the cured fibers under an inert atmosphere at high temperatures. Fine-diameter continuous SiC fibers are finally obtained from polycarbosilane precursors. Nippon Carbon Co. first realized the industrial production of a series of continuous SiC fibers under the trademark Nicalon. Compared with CVD SiC fibers, the biggest advantage of PPD SiC fibers is their much smaller diameter, which allows easy weaving into a variety of fabrics. It can then be easily used as reinforcements in complicated composites. In addition, PPD SiC fibers are very good heat-resistant materials and can be used as insulation materials, high-temperature conveying belts, melt filters:

Top View

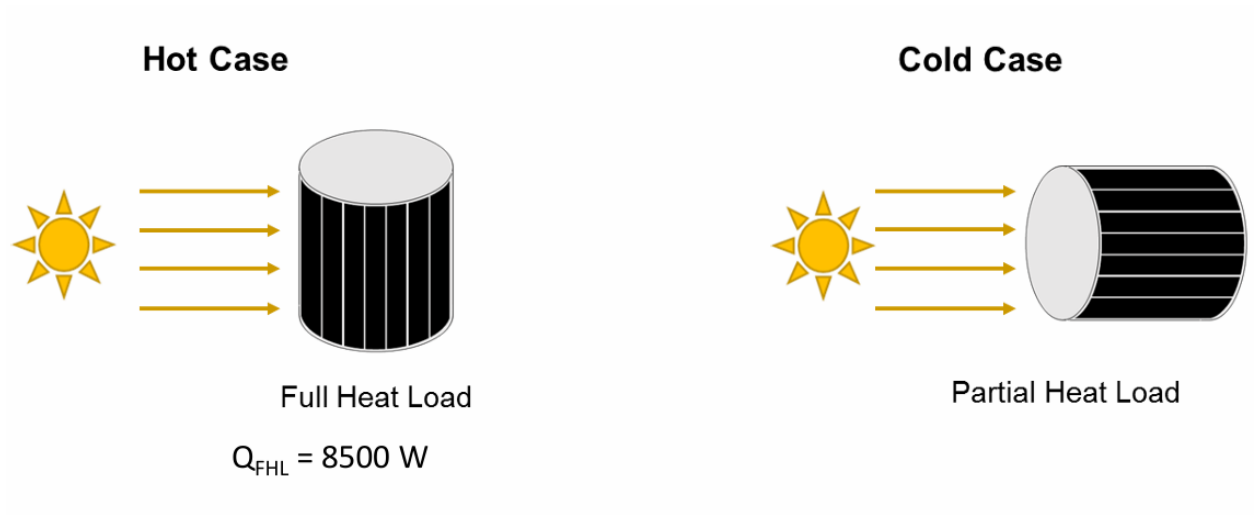


Body-mounted radiators
that are discretized into N
 $= 360$ panels

Side View



Each panel is discretized into K
blocks, each with their own
independent emissivity



A-glass fiber, containing high alkali metal oxides; C-glass fiber, resistant to chemical attack; D-glass fiber, with a high dielectric property; E-glass fiber, with high electric insulation; M-glass fiber, with a high Young's modulus; S-glass fiber, with a high tensile strength; AR-glass fiber, alkaline resistant and suitable for reinforcing cement matrix composites. As reinforcements, glass fibers can be processed into yarns, cloths, belts, as well as three-dimensional fabrics, such as carpets;

```

glass_A:
SiO2 = 72
B2O3_min = 0.6
B2O3_max = 1.5
CaO = 10
Na2O = 14.2
MgO = 2.5
others = -

glass_C:
SiO2 = 65
Al2O3 = 4
B2O3 = 6
Na2O = 14
CaO = 8
others = 3

glass_D:
B2O3 = 0.3
others = -

glass_E:
SiO2 = 52
others = -

glass_E_CR:
SiO2_min = 58

```

```

SiO2_max = 63
Al2O3_min = 10
Al2O3_max = 13
B2O3_min = 1.0
B2O3_max = 2.5
CaO_min = 21
CaO_max = 23
others_max = 1.2

glass_M:
SiO2 = 53.7
SO3 = 0.7
LiO2 = 0.5
SiO2_alt = 56
Al2O3_min = 12
Al2O3_max = 16
B2O3_min = 5
B2O3_max = 13
CaO_min = 16
CaO_max = 25
TiO2_min = 1.0
TiO2_max = 2.5
ZnO_max = 3.5
ZrO2 = 2.0
BeO2 = 8.0
CeO2 = 3.0
TiO2_extra = 8.0
others_min = 0.0
others_max = 2.0

glass_S:
SiO2 = 65
Al2O3 = 25
others = 10

glass_ZorAR:
SiO2 = 71
CaO = 11
ZrO2 = 16
TiO2 = 2

```

Applications of Advanced Composite Materials in Aircraft Structures In the USA and Europe, development of advanced composite materials began in the 1960s and was first applied in the early 1970s. Fighter jets in service in the 1980s used advanced composite materials in their wing and tail structures, comprising 20-30% of the total aircraft weight. The wing structures of the stealth B-2 developed in the 1980s was made up of *60% composite materials. Applications of advanced composite materials in civil aircraft proceeded more cautiously because of safety and cost considerations. To promote confidence in

composite technologies for civil aerospace applications, many programs were implemented in the USA in the 1970s. These include the Aircraft Energy Efficiency (ACEE) and Advanced Composite Technology (ACT) programs, and the Composite Affordability Initiative (CAI). In Europe, the Technology Application to the Near-Term Business Goals and Objectives (TANGO) project was initiated with the aim of producing composite wing and fuselage components at a competitive cost. In the recently launched A380, A350, and Boeing 787, contributions of advanced composite materials to the structural weight were 22, 52, and 50%, respectively.

Structural Performance (1) Specific strength and specific modulus Carbon fiber/epoxy resin composites are most often used in aircraft structures. The use of these materials can greatly reduce the structural weight because of their high specific strength (rb/q) and specific modulus (E/q). laminated structures, prepared by unidirectional prepreg laying-up and curing, are the main materials used in aircraft structures. Unidirectional prepreg tapes are strongly orthotropic, i.e., performance in the fiber direction is different to that vertical to fibers. To satisfy the performance requirements in specific directions in a structural plane, it is necessary to place unidirectional tape in different directions at certain ratios. The designed laminates may be either isotropic or anisotropic and may be either symmetrically balanced or asymmetrically balanced. This unique feature offers considerable flexibility to designers. The use of low-density advanced composite materials requires new structural design methods to be applied at an early stage to fully take advantage of the properties of composite materials. Composite forward-swept aircraft wing and the zero thermal expansion coefficient structures are typical applications of laminating anisotropy, which offers tailorable performance.

Damage, fracture, and fatigue behavior Features of advanced composite materials often include anisotropy, brittleness, and inhomogeneity. These features, and the inferior interlaminar properties compared with those in-plane, cause the failure mechanisms of laminate composites to be very different from those of metals. Their damage, fracture, and fatigue performances are also very different. Although the laying-up and autoclave processing used for composite components is simple, impacts by foreign objects during machining and delivery are more likely to damage or induce defects in composite parts than equivalent metal parts. Table 4.2 summarizes the fatigue and damage tolerance of metal and composite structures.

1. Main defect/damage types: Cracks are the main damage mode of metal structures. For composite structures, the critical defect/damage modes include interlaminar debonding, delamination, and low-energy (low-speed) impact damage. Impact damage can cause critical damage to composites by significantly decreasing their actual compression load-bearing ability. While no visible damage may be apparent from inspection of the outer surface, impacts may induce cracking of the internal matrix or delamination. Visible checks are only reliable once the compression strength has decreased to 40% of its original value after an impact. Delamination is a unique damage mode of laminated composites. Impacts from tools, and foreign bodies such as runway chippings, hailstones, and birds, together with the local interlaminar stress concentration and over-loading, may all contribute to internal delamination.

Metal:

Main damage is due to fatigue, corrosion, and stress corrosion; critical damage is cracking under tensile loads; behavior shows yielding in stress-strain; notch sensitivity is small and static strength is insensitive; fatigue resistance is insensitive; damage check before failure is impossible visually; damage grows along main crack with regularity.

Composite:

Main damage caused by foreign impacts and processing defects; critical damage is impact-induced delamination under compression; stress-strain is linear until sudden final failure; notch sensitivity is very high and static strength shows large dispersion; fatigue resistance is very sensitive; damage can be visually detected before failure; damage grows as multi-damage propagation without regularity.

For composite matrices, high-performance resin systems must satisfy the requirements of practical engineering applications including processing ability, thermal, physical and mechanical properties. The processing performance of resin matrices will include their dissolution in solvents, melting viscosity (flow ability) and change in viscosity behavior (processing windows). The thermal resistance includes the glass transition temperature (T_g), thermal-oxidation stability, thermal decomposition temperature, flame-retardant performance and thermal deformation temperature, which can dominate the composite service temperature ranges. The discussion about the mechanical properties of resin matrices will cover their property specifications under service conditions such as tensile strength, compression, bending properties, impact resistance and fracture toughness. Resin matrices should have very good electric properties and chemical resistance including solvent resistance, self-lubrication and anti-corrosion properties.

Black holes have an extreme environment to probe these composite materials: A particle in a curved spacetime moves along a time-like geodesic. If u is its velocity, the equation of motion is $\nabla u u = 0$, or equivalently, $u^\alpha \nabla_\alpha u^\mu = 0$

Evaluate the behavior of materials such as SiC fibers (Nicalon), glass fibers (types E, M, S, etc.), and composites (carbon/epoxy, high-temperature polymers) under conditions of:

1. High electromagnetic radiation (X-ray, gamma ray, extreme UV)
2. Temperature gradients exceeding 2500°C
3. Simulated gravitational acceleration ($\sim 10^6$ to 10^8 g)
4. Stress from shock waves or Hawking-type impulses/gravitational radiation

$$U^\mu \nabla_\mu n = 0$$

This system can be represented with tensors in Schwarzschild or Kerr space (rotation). You can simulate a falling particle/material sample and obtain:

- Induced stresses (tidal forces)
- Spaghettification effects
- Energy gradients

Thermal Resistances (1) Glass transition temperature The glass transition is a secondary transition in which polymers will transit from a glass state into an elastic state. At temperatures lower than the glass transition temperature, polymers will be subject to a series of changes including sudden changes in specific heat and capacity, movement of molecular chain segments and the fast growth of linear expansion coefficients. In polymer chains, the existence of strong polar groups will increase the interaction forces between molecules, which further increases chain densities, and as a result, polar polymers will possess a higher Tg. In polymer main chains and side groups, huge rigid groups can inhibit chain segment free rotation, which is useful for an increase in Tg, while flexible side groups can increase the distance between chains and allow them to move more easily, resulting in a decrease in Tg. Therefore, to increase the Tg and the thermal resistance the resin matrices of advanced composites will normally be designed to contain a large quantity of chains with huge rigid groups. the equation of motion in the standard form $d^2x^\mu/d\tau^2 + \mu v^\lambda dx^\nu d\tau dx^\lambda d\tau = 0$.

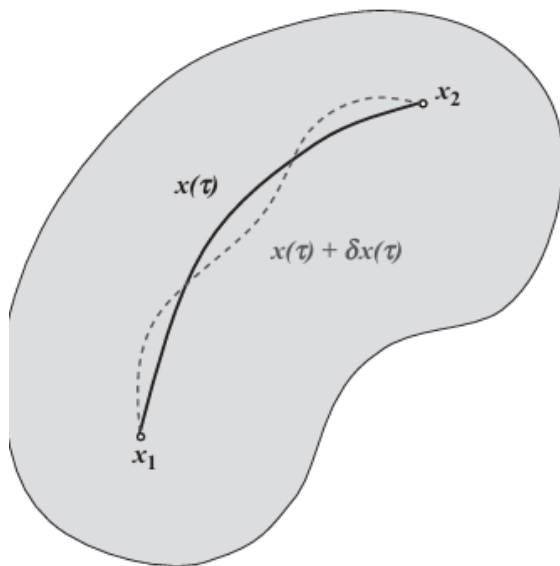


Fig. 4.1 The geodesic line between points x_1^μ and x_2^μ and the variation around it.

Hamiltonian form of the equation of motion The Hamiltonian $H = p^\mu dx^\mu d\tau - L$, $p^\mu = \partial L / \partial \dot{x}^\mu$. The corresponding action in the Hamiltonian form is $\tilde{S}H[x^\mu(\tau), p^\mu(\tau), \eta(\tau)] = \int d\tau (p^\mu \dot{x}^\mu - H)$.

The most stable polymers are ladder polymers composed of heterocyclic and aromatic conjugate structures. The most stable flexible chain groups are aliphatic compounds in which all the hydrogens are substituted by fluorine and phenyl. $-O-$, $-S-$, $-CONH-$ and $-CO-$ can also give good thermal-oxidant stability; $-SO_2-$, $-NH-$, hydroxyl and chloride groups impart lower thermal oxidation stability. The thermal-oxidation stability of xylene-containing polymers increases as follows: $p > m > o$. Generally, cross-linking can improve polymer thermal-oxidant stability.

It might be an interesting point to adapt the polymers & carbon fiber reinforcement composites to the black hole conditions in order to build systems such as the solar parker probe.

Coefficient of Thermal Expansion (CTE)

The combination of two materials with different CTE will cause interface stress when the temperature changes. If this difference in CTE is large, the interfacial bond can be damaged. Composites are composed of resins and reinforcing fibers. Stress can be generated at the resin and fiber interface as the temperature changes, possibly resulting in delamination by severe stresses. Adhered structures are also easily damaged at the adhering interface. Therefore, for high-performance resin matrices, CTE matching of reinforcing materials should be seriously taken into account. CTE can be determined by thermal mechanical analysis (TMA).

In general, inorganic materials have a lower CTE than polymeric materials. To decrease the CTE of polymers, the following methods can be adopted: (1) Introduce ordered structures such as crystals into the polymers. (2) Use huge rigid structures like aromatic heterocyclic structures to reduce polymer molecular segment movement. (3) Increase cross-linking density.

A. Material Variables:

Fiber type (E-glass, SiC, S-glass, etc.)

Chemical composition (SiO₂, ZrO₂, TiO₂)

Morphology (filament diameter, braid shape)

B. Physical Variables:

gsimg

Sim = simulated gravity (by centrifugal acceleration or Kerr metric)

ΦradΦ

rad = radiative flux (W/m²)

Tmax

Tmax= maximum exposure temperature

τvidat

life= half-life under radiation and load

σfractσ

fract= critical fracture stress

Module: Heat Transfer in Solids
Add: Surface Heat Source with $\lambda = \lambda_{\text{radiation}}$
Radiation type: Directional Beam
Intensity Profile: Gaussian or Blackbody

Resin Matrix	Tensile Strength (MPa)
---------------------	-------------------------------

-------	--

Polyetheretherketone (PEEK)	99
Polyetherimide (PEI)	107

Thermoplastic polyimide (PI(TP))	87
Bismaleimide (BMI)	145
Thermosetting polyimide (PI(TS))	148
Epoxy	134
 Bending Strength (MPa)	 Bending Modulus (GPa)
<hr/>	<hr/>
PEEK	84
PEI	75
PI (TP)	85
BMI	45
PI (TS)	40
Epoxy	50

High-performance resins are increasingly used in the electronics industry as insulating materials and wave transparent materials. Therefore, understanding the electric properties of high-performance resins is of great significance. For engineering materials, the electric properties of interest are the dielectric properties and the electric breakdown intensity. The dielectric constant of materials is the storage of energy in a unit material volume under a unit of electric field intensity. The magnitude of the dielectric constant is related to the extent of dielectric polarization (electronic polarization, atom polarization and orientation polarization). For polymeric materials used in insulating applications, their insulating performance should be considered in addition to their satisfied thermal resistance and mechanical properties. For example, when the heat generated by dielectric loss under a certain electric field exceeds the material's dispersed heat, local overheating will be induced and subsequently cause a breakdown in materials. The deformation of polymers under stress can also affect the breakdown behavior causing a decrease in the breakdown intensity. This kind of breakdown behavior, under these circumstances, is referred to as electric-mechanical breakdown.

Resin Matrix	Electric Breakdown Intensity (V/mil)	
<hr/>		
Epoxy	400	
Nylon 6	385	
Polyester	300–400	
Cyanate Acid Ester	390	
BMI	400	
Polyethylene	480	
 Dielectric Constant (60 Hz)	 Dielectric Loss Tangent (60 Hz)	
<hr/>		
Epoxy	4.02–4.79	0.005–0.038
Nylon 6	4.0–5.3	0.014–0.06
Polyester	2.8–4.4	0.003–0.04
Cyanate Ester	2.7–3.2	0.001–0.005
BMI	4.0–4.8	0.004–0.035

Polyethylene 2 . 3 <0 . 0005

Note: 1 mil = 25 . 3 μm

Black holes: functionals of worldlines $x^\mu(\tau)$ connecting two points, the initial one $x^\mu_1 = x^\mu(\tau_1)$ and the final one $x^\mu_2 = x^\mu(\tau_2)$. Now we consider the same actions but from a different point of view. We fix the initial point x^μ_1 but keep the final point x^μ_2 arbitrary. We calculate the value of the action as a function of the final point, assuming that the equations of motion are satisfied. We fix the gauge choice by putting $\eta = 1$, so that τ is a proper time (or affine) parameter. We denote the obtained function by $S(x_2)$. For simplicity, we omit the index 2.

we obtain $\delta S = p_\mu \delta x^\mu$

Composite-Matrices:

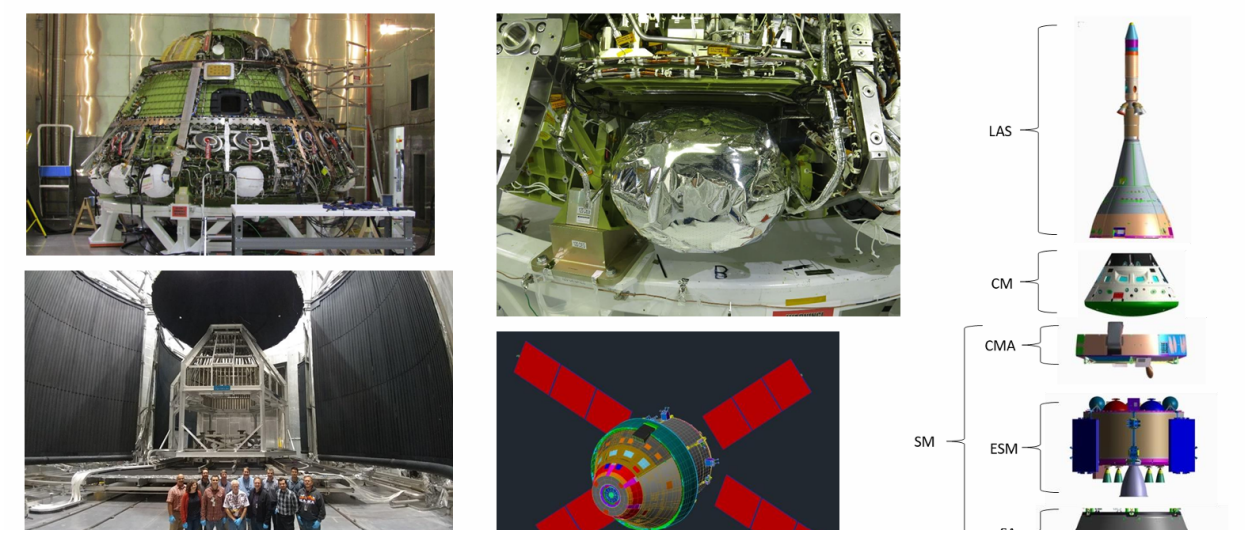
Differential scanning calorimetry (DSC) and differential thermal analysis (DTA) are most commonly used to characterize the curing behavior of resin matrices. They can measure and monitor the reaction heat and temperature in the curing reactions of the composite resin matrices and can also characterize resin decomposition and oxidant degradation. For composite resin matrices, DSC and DTA primarily determine reaction parameters such as curing reaction onset and peak temperatures, reaction enthalpy and peak shape. Both DSC and DTA can be used for isothermal and dynamic (constant heating) operation models. For the heating and curing processes, composite resin matrices will undergo state changes from solid to flow states because of the application of heat. A change back to the solid state will result from resin curing, and this will cause significant changes to the resin's dielectric properties. Dynamic dielectric thermal analysis (DETA) can be used to characterize the curing behavior by allowing the determination of cure temperatures. For reactions with mass changes, TGA can be used to study the curing processes. For example, the phenolic resin curing reaction depends upon the imidization of polyimide resins.

Extreme conditions for a black hole: Using an electric arc furnace in an inert atmosphere to reach temperatures of 2500–3000°C

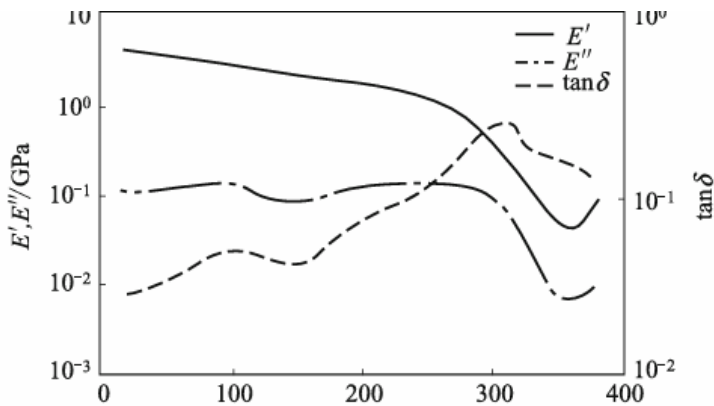
X-ray/gamma bombardment (simulated with a high-energy pulsed laser)

High-acceleration centrifuge (simulated 10,000–20,000 g) to approximate gravitational tidal wave

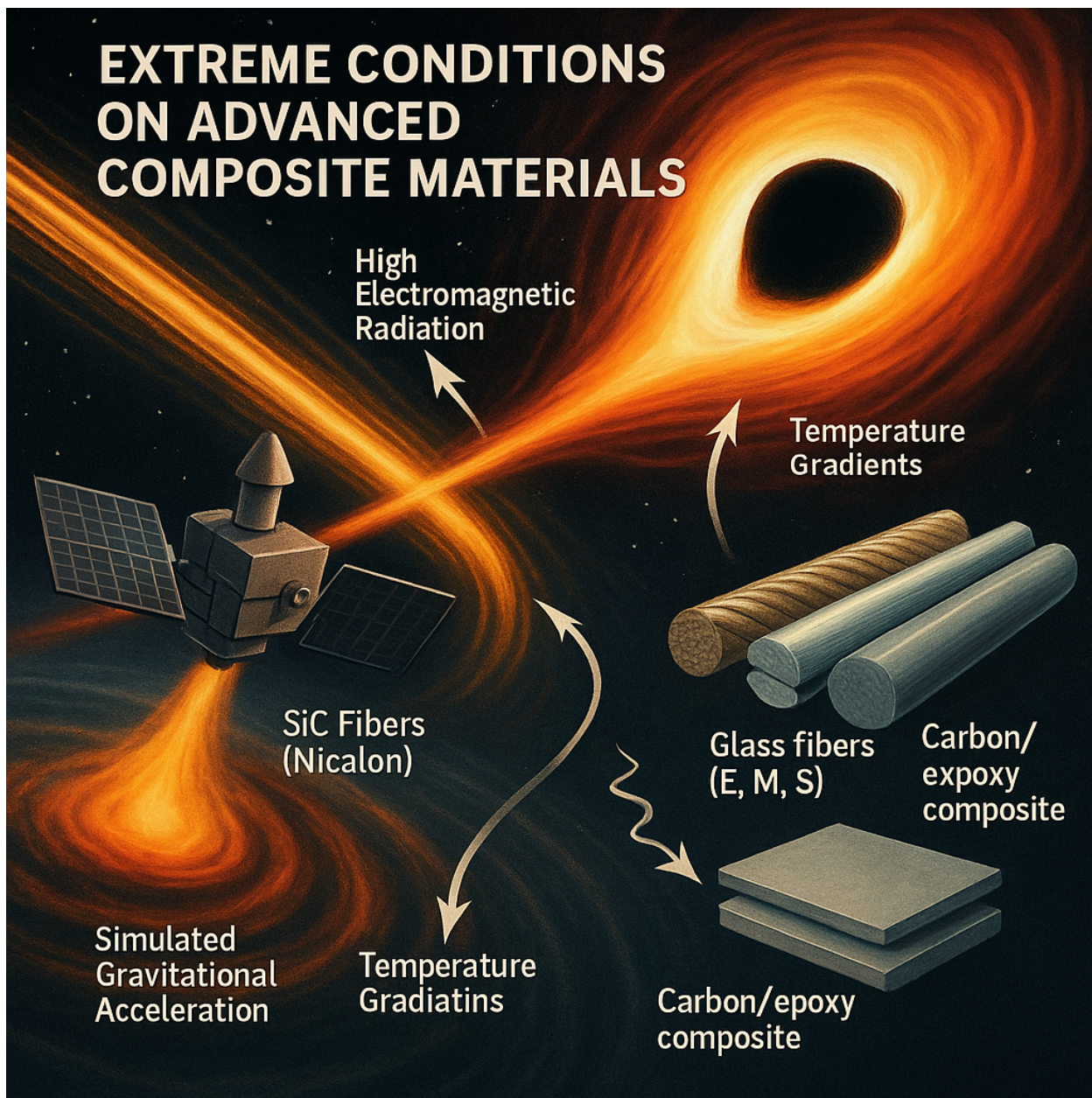
Optical camera simulating gravitational lensing in fiber optics



In the FTIR method, the resin curing degree is determined by the relative intensity changes in the characteristic peaks of the reacting groups in the resin system before and after curing. For this method, two basic requirements have to be met: One is that the characteristic peaks of the reacting groups should not be influenced by other group characteristic peaks and the other is that there should be a proper and stable reference standard peak on the resin's infrared spectrum. The standard peak should be independent of other group characteristic peaks. For example, in epoxy resin curing the epoxy group's characteristic peak is at 915 cm^{-1} and the benzene ring peak is at 1500 cm^{-1} ; this peak can be used as the reference standard peak. These two peaks can be represented by S915 and S1500, and $S915/S1500$ is thus the relative intensity of the epoxy group's peak. Before and after curing, the epoxy group will give the relative intensities of $(S915/S1500)_0$ and $(S915/S1500)_t$, and the resin curing degree α will be: $\alpha = \sqrt[4]{(S915/S1500)_t / (S915/S1500)_0}$. Since reaction heat will be released during the resin curing process and the curing reaction heat is proportional to the resin curing degree, the curing degree can be determined by thermal analysis to also give the residual heat of the cured resin: $\alpha = \sqrt[4]{DH_t / DH_0}$ where DH_0 is the total released reaction heat and DH_t is the reaction heat over a certain curing time.



EXTREME CONDITIONS ON ADVANCED COMPOSITE MATERIALS



Consider a foliation of the spacetime by a one parameter set of 3-dimensional surfaces . We assume that these surfaces are space-like and their equation is $t(x\mu)=\text{const}$. Let y_i ($i = 1, 2, 3$) be coordinates on t . For a given foliation equation $y_i = y_i(t)$ determines the trajectory of a particle. We denote $U = -g_{tt}$, $A_i = g_{ti}$, $V = g_{ir}rA_j + U$

Composites Carbon-Carbon: Resin matrices and thermoplastic (crystallized or half-crystallized) polymers need to absorb ambient heat upon melting. Therefore, thermal analysis (DSC and DTA) can be used to determine the melting points of resin monomers and thermoplastic resins. In these analyses, resin melting points and melting heat can be determined. The related standard method is ASTM E794. Softening points are also an important physical parameter of resins with non-crystallized solids or half-solid states. These types of resins include solid epoxy resins and phenolic resins. National standard GB/T 12007.6-1989

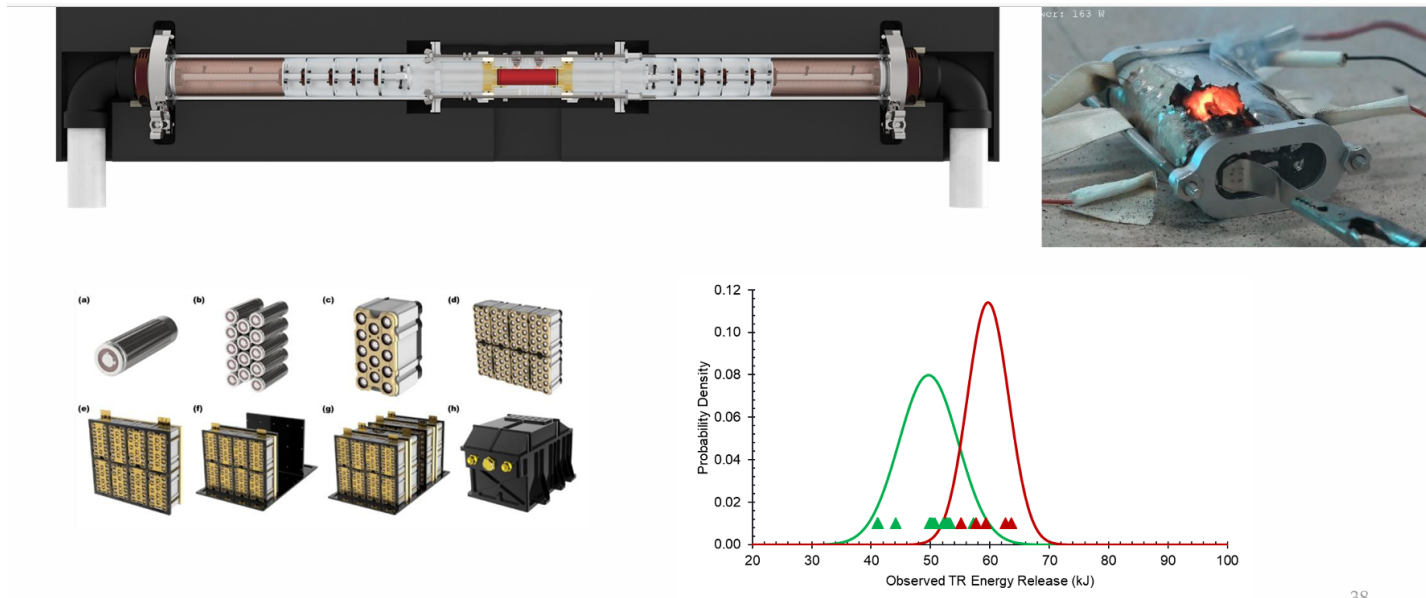
specifies the “ring-and-ball” method to determine resin soft points (especially for epoxy resins) as follows: evaluate the resins in a horizontal copper ring under the action of a steel ball in a water bath or in a glycol alcohol bath heated at a specified rate and determine the temperature where the steel ball fell by 25 mm.

The water absorption test conditions for different materials can be determined based on the required service, for example, for high-temperature curing and high-performance resin matrices, general hot/wet test conditions will be boiling water ($97^{\circ}\text{C} \pm 2^{\circ}\text{C}$) for 48 h. For medium-temperature curing systems, the general test conditions will be water immersion or R.H. environmental exposure. Detailed test methods and conditions can be found in the standard GB/T 1034-1998. The resin matrix coefficient of thermal expansion (CTE) can be determined by measuring specimen length changes under a specific temperature difference and calculating the changes in length before and after. Detailed testing, calculation methods and equipment principles can be found in GB/T 1036-1989.

The Characterization of resin thermal resistance The thermal resistance of composite resin matrices is usually characterized by the glass transition temperature (T_g) and the thermal deformation temperature. Theoretically, all the obvious changes or the sudden physical property changes taking place during the glass transition processes can be used to measure the glass transition temperature of polymer materials. Currently, the instruments or devices used for polymer glass transition temperature measurement rely on physical property changes in polymers including volume changes, thermal dynamic property changes, mechanical changes and electric–magnetic property changes. A black hole with very low mass—the idea is interesting. In theory, a primordial black hole (the kind hypothesized to have existed at the beginning of the universe) could have a small mass and a less extreme event horizon. However, we have yet to detect one. Another concept is the artificial micro-black hole, a possibility that has been discussed in theoretical physics. If they could be created and stabilized, they could be used to generate controlled curvature of spacetime without destroying a spacecraft. Considering artificial or natural gravitational structures, you could perhaps look at models of space-time curvature in advanced relativistic physics. There are studies on how to manipulate these forces, although we're still far from achieving anything practical.

The Granoc XN series are a kind of low modulus, low strength carbon fiber with a fiber diameter of about 10 lm, a Young's modulus of 55–155 GPa and a tensile strength of 1.10–2.40 GPa. However, their density is low at 1.65–2.80 g/cm³ and their tensile strain is relatively high at 1.5–2.0%. They are mainly used for civil engineering and infrastructure in the form of sealing materials, reinforcing sheets for repairing concrete, tunnel walls and poles. The Granoc CN series are a kind of carbon fiber mainly used for recreational sport supplies and general industrial applications. Compared with T300-type PAN-based carbon fibers, their Young's modulus is much higher and applicable to materials requiring stiffness. They can be used in electronic equipment, precision optical instruments, acoustics and audio equipment, robot arms and various rollers. The Granoc YSH series of carbon fibers are mainly used in the manufacture of satellite antennas, satellite structure components, solar panels, joysticks, stings, missile components and rocket components. In China, researchers mainly focus on common pitch-based carbon fibers using an isotropic pitch as the precursor as well as high-performance pitch-based carbon fibers using mesopitch as the precursor. The common carbon fibers have been continuously prepared with a tensile strength of 0.80–0.95 GPa, a Young's modulus of 40–45 GPa and a tensile strain of 2.0–2.5%, but these have not yet

been industrialized. Because of their poor mechanical properties, they are mainly used for functional or cement matrix composites. High-performance pitch-based carbon fibers are prepared from mesopitch by melt spinning, pre-oxidation, carbonation and graphitization [19]. Their performance depends largely on the structure and composition of the precursor. Mesopitch has been studied in-depth, and at the end of the last century, graphite fibers were produced by the modification and modulation of oil residue and coal. Spinnable pitch has a softening point of 264–278 °C and a meso pitch content above 95%.



What's out there in space that we could exploit?

If we're looking for astrophysical objects with manageable gravitational fields that won't destroy a spacecraft, we might consider:

White Dwarfs and Neutron Stars

These compact stars generate intense gravitational fields, but they're much less destructive than black holes. Harnessing the curvature of their spacetime could be viable for advanced gravitational assists.

Low-Interaction Supermassive Black Holes

Giant black holes exist at the centers of galaxies, whose zones of influence are vast but not necessarily deadly in all regions. If a stable point were found near their outer event horizon, their effects could be harnessed without falling into them.

Natural Gravitational Lenses

Some galaxy clusters generate gravitational lenses that bend light and affect the trajectory of nearby objects. If this were used in a ship's structural design, it could allow for gravitational deflections without the need for fuel.

Using existing anomalies in the galaxy

If building a gravitational drive is too difficult, we could perhaps use gravitational structures already present in the universe.

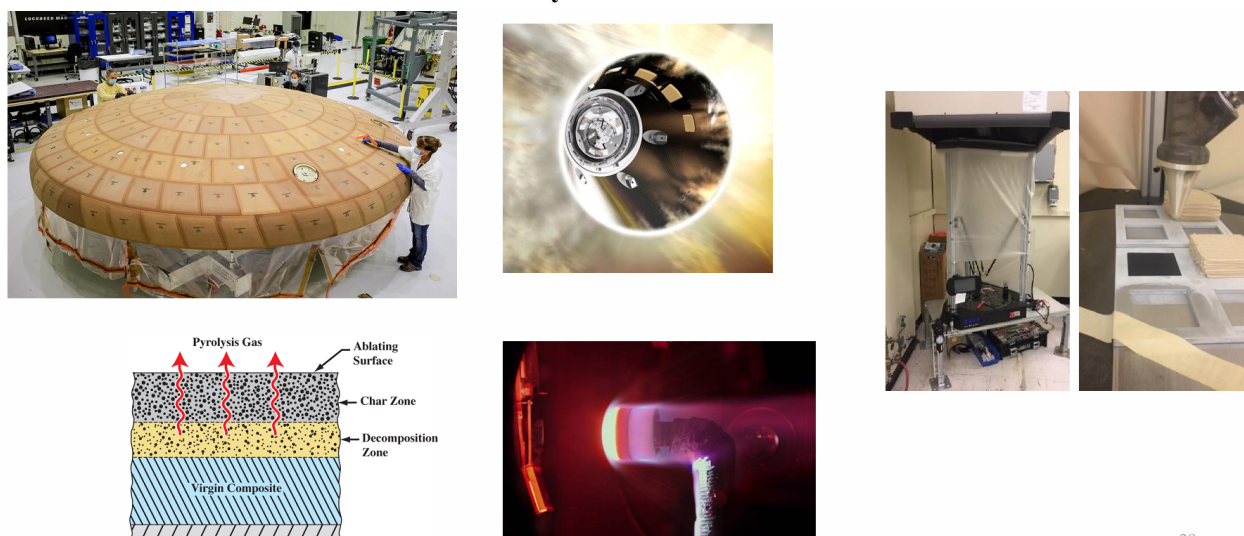
1. Wormholes or gravitational lenses: If we can find a point in space with useful gravitational effects, we could use them to accelerate spacecraft without the need for traditional fuel.

2. Orbits around neutron stars: The gravitational curvature around certain extreme bodies could allow for energy-efficient maneuvers.

3. High-density confined plasma: If plasma could be confined in a smaller reactor with ultra-efficient magnetic fields, we could obtain a useful energy source for continuous propulsion.

Interaction between electromagnetic and gravitational fields: Some models of quantum gravity speculate how gravitational fields can be generated by extreme energy fluctuations. Perhaps, if a small gravitational vortex could be stabilized, a reactionless engine could be achieved.

Orion and 3D Printed Thermal Protection Systems:



Thermal control phase change materials

Need higher latent heat of fusion materials and PCM architectures that lead to high energy absorption per storage volume solutions on spacecraft.

High-performance, low contact pressure thermal interfaces

Need thermal interfaces with predictable and repeatable interface conductances in different environments (lab versus spacecraft). Spacecraft applications typically cannot apply high pressure.

- High power density, long lifetime, space-qualified heater systems Need robust high watt density heaters, especially for non-planar surfaces.
- Full-field, Full Structure Instrumentation Need instrumentation for stagnant fluid lines, high stress areas on structure, and high temperature structures.

```
CarbonFiber1: Diameter=13.25µm, TensileStrength=2.31GPa (C.V.=20.72%) ,  
YoungModulus=525.6GPa (C.V.=17.0%) , TensileStrain=0.44% (C.V.=18.6%)
```

```
CarbonFiber2: Diameter=13.68µm, TensileStrength=2.18GPa (C.V.=22.70%) ,  
YoungModulus=483.2GPa (C.V.=9.95%) , TensileStrain=0.46% (C.V.=22.5%)
```

```
YShaped1: EqDiameter=35.5µm, OxidationGas=Air, Temp=300°C, Time=2.0h,  
TensileStrength=0.882GPa
```

```
Circular1: EqDiameter=34.9µm, OxidationGas=O2+Air, Temp=240°C, Time=-,  
TensileStrength=-
```

```
YShaped2: EqDiameter=27.5µm, OxidationGas=Air, Temp=300°C, Time=10.0h,  
TensileStrength=0.607GPa
```

```
Circular2: EqDiameter=29.6µm, OxidationGas=Air, Temp=240°C, Time=24.0h,  
TensileStrength=0.603GPa
```

Other system propulsion variables to consider:

As gases expand in the nozzle, their temperature and pressure change.

The shape of the nozzle influences flow efficiency.

Some chemical species can condense if the temperature drops sufficiently.

The effect of particles in the gas mixture is considered, as they can reduce flow efficiency.

Losses due to gas viscosity at the nozzle walls are studied.

Computational methods for calculating propellant efficiency are analyzed.

Technical Component	Function	Material / Details
Front Heat Shield coating	Protection against extreme solar radiation	Carbon-Carbon + ceramic
Adjustable Solar Panels	Electrical Power	Monocrystalline silicon with thermal reflective film
Propellant Tanks high-silica fiberglass	Fuel storage (hydrazine, xenon)	Titanium, protected by
Ion Propulsion System	Orbital correction, navigation	Tungsten alloys, electromagnetic acceleration system
AI System for Data Mining quantum FPGA	Collection, analysis, and prioritization	Rad-hard CPU with optional
Plasma & Magnetic Sensors encapsulated sensors	Study of solar and deep-space particles	Insulating ceramic casing,
Structural Exoskeleton embedded in epoxy matrix	Protection and mechanical support	M-Glass + carbon fibers
Cooling System pipes	Heat distribution and dissipation	Closed coolant circuit + heat
Communication System dielectric-coated antennas	Link with ground stations & spacecraft	High-gain,
Redundant Flight Computer (e.g., FreeRTOS, QNX)	Trajectory, propulsion, and data control	Microcontrollers with RTOS
Cameras & Spectrometers E-glass & fused silica lenses	Image capture and spectral analysis	Radiation shielding with

Variation of constituent properties: The non-uniformity of constituent materials results in a certain scatter of their performance. The performances of composites not only depend on their constituent materials, but also the combination of constituents.

1. Instability of processing techniques: Knowledge is limited on the physical and chemical mechanisms currently used to prepare composite materials. This results in poor reproducibility of processing and a large scatter in the performance of materials.

2. Imperfectness of testing methods: As a relatively new kind of material, currently there are no suitable methods and standards to test and inspect certain properties of composites. In the established standards, specimens cannot perfectly reflect the real-world performance of composite structures. There is much work required on evaluating composite stability by nondestructive testing.

3. Lack Of Statistical data: Compared with traditional materials, data on composite

performances are severely limited. In many databases, typical values are given with insufficient statistical data.

4. Lack of knowledge about the regularity of changes in composite material properties over time: Composite matrices are very sensitive to time- and temperature-dependent effects and their performances will change with time.

Current accumulated data still does not reflect the behavior of composites over a full range of ambient conditions and different time periods.

Black hole context image:

Equations of Motion 113

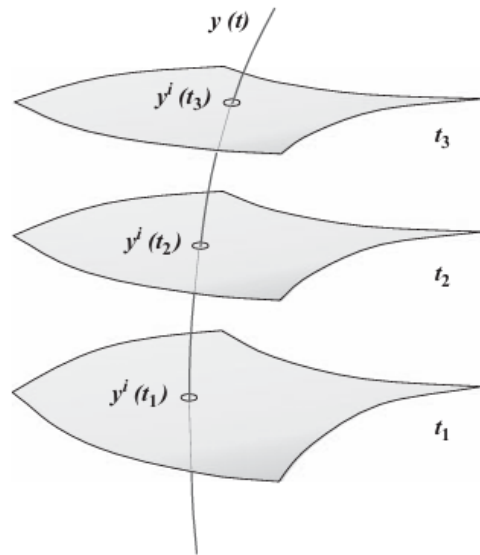


Fig. 4.2 The foliation of the spacetime by a set of 3-dimensional space-like surfaces Σ_t .

Need instrumentation to obtain flight vehicle performance data such as:

- Pressure
- Temperature
- Heat flux
- Radiation
- Spectra from mid-IR to VUV
- Strain
- TPS recession/in-depth response

